Article

Not peer-reviewed version

Divergent Transcriptional Regulation and Functional Role of Chick WT1_76127 and Mouse Gm14014 lncRNAs in Epicardial Cell Migration

Sheila Caño-Carrillo , Carlos Garcia-Padilla , Amelia E Aranega , Estefanía Lozano-Velasco , Diego Franco *

Posted Date: 2 August 2024

doi: 10.20944/preprints202408.0067.v1

Keywords: lncRNAs; epicardial cell; cytoskeletal remodelling; cell migration

doi:10.20944/preprints202408.0067.v1

Article

Divergent Transcriptional Regulation and Functional Role of Chick WT1_76127 and Mouse Gm14014 lncRNAs in Epicardial Cell Migration

Sheila Caño-Carrillo [1], Carlos Garcia-Padilla [1], Amelia E Aranega [1,2], Estefania Lozano-Velasco [1,2] and Diego Franco [1,2,*]

[1] Cardiovascular Development Group, Department of Experimental Biology, University of Jaen, 23071 Jaen, Spain
[2] Fundación Medina, 18016 Granada, Spain
* Correspondence: dfranco@ujaen.es

Abstract: Cardiac development is a complex developmental process. The early cardiac straight tube is composed of an external myocardial layer and an internal endocardial lining. Soon after rightward looping, the embryonic heart becomes externally covered by a new epithelial lining, the embryonic epicardium. A subset of these embryonic epicardial cells migrate and colonize the embryonic myocardium, contributing to distinct cell types. In recent years, our understanding of the molecular mechanisms that govern proepicardium and embryonic epicardium formation has greatly increased. We have recently witnessed a novel layer of complexity governing gene regulation with the discovery of non-coding RNAs. Our laboratory recently identified three distinct lncRNAs, adjacent to the *Wt1*, *Bmp4* and *Fgf8* chicken gene loci, with enhanced expression in the proepicardium that are distinctly regulated by Bmp, Fgf and thymosin β4, providing support of their plausible implication in epicardial formation. Expression of lncRNAs was analyzed in different chicken and mouse tissues as well as their subcellular distribution in chicken proepicardial, epicardial, ventricle explants and in different murine cardiac cell types. lncRNA transcriptional regulation was analyzed by using siRNAs and expression vectors of different transcription factors in chicken and mouse. Antisense oligonucleotides were used to inhibit *Gm14014* expression. Cardiac injury was induced *ex vivo* in mouse ventricle explants by cryoinjury. Furthermore, RT-qPCR, immunocytochemistry, RNA pulldown, Western blot, viability and cell migration assays were conducted to investigate the biological function of *Wt1_76127* and *Gm14014*. We demonstrated that *Wt1_76127* in chicken and its evolutionarily conserved homologue *Gm14014* in mice are widely distributed in different embryonic and adult tissues and distinctly regulated by cardiac enriched transcription factors, particularly *Mef2c* and *Nkx2.5*. *Gm14014* is distinctly regulated in mouse ventricular cryoinjury *ex vivo* models, displaying a negative correlation with epicardial and epithelial to mesenchymal transition markers. Furthermore, silencing assays demonstrated that mouse *Gm14014*, but not chicken *Wt1_76127*, is essential for epicardial, but not endocardial or myocardial cell migration. Such process is governed by partnering with Myl9, promoting cytoskeletal remodeling. Our data evidence that Gm14014 plays a pivotal role in epicardial cell migration essential for heart regeneration.

Keywords: lncRNAs; epicardial cell; cytoskeletal remodelling; cell migration

1. Introduction

Cardiac development is a complex developmental process that initiates soon after gastrulation with the configuration of symmetrical pools of cardiomyogenic precursors that subsequently fused in the embryonic midline, leading to the formation of the cardiac straight tube [1]. This early tube is composed of an external myocardial layer and an internal endocardial lining. Soon after, a rightward looping develops and embryonic atrial and ventricular chambers become progressively configured [2]. At this stage, the embryonic heart becomes externally covered by a new epithelial lining, the embryonic epicardium (EE). The EE originates from the proepicardium (PE), a transitory structure with a cauliflower appearance located at the junction of the cardiac and hepatic anlagen within the *septum transversum* [3]. Cells emanating from the PE bridged to the naked embryonic myocardium providing an external lining [4]. Soon after, a subset of these embryonic epicardial cells, undergoes an epithelial-to-mesenchymal transition (EMT), colonizing the subepicardial space and migrating into the embryonic myocardium [5,6]. In chicken, these epicardial derived cells (*i.e.* EPDCs) have been consistently reported to contribute to distinct coronary vascular components, including vascular endothelium, smooth muscle and adventitial layers, as well as cardiac fibroblasts [7,8]. However, in mice, several lineage tracing experiments have provided evidence of a modest contribution of EPDCs to cardiac endothelium, while their contribution to coronary smooth muscle and adventitial vasculature and fibroskeleton is undisputed [9].

In recent years, our understanding of the molecular mechanisms that govern proepicardial and epicardial formation has greatly emerged [3]. Evidence highlighting the pivotal role of Bmp and Fgf during proepicardial and myocardial specification was reported by Kruithof *et al.* [10] demonstrating that Fgf enhances proepicardial specification while Bmp promotes cardiomyogenic differentiation. More recently, the role of distinct transcription factors has emerged as key players in epicardial development. *Wt1* is essential for epicardial EMT and maturation [11–16]. Similarly, *Tbx18* has also been reported to be expressed in the embryonic epicardium but its role in epicardial formation is controversial. Greulich *et al.* [17] reported that *Tbx18* is dispensable for epicardial formation, EMT and subsequent differentiation into smooth muscle cells and fibroblasts while Wu *et al.* [18] demonstrated impaired coronary plexus formation and identified impaired expression of several signaling pathways related to vascular development, such as Hedgehog, Vegf, Angiopoetin and Wnt signaling. Further support for the role of *Tbx18* in epicardial EMT was reported by Takeichi *et al.* [19] using murine primary epicardial cells. *Epicardin/Tcf21* is also discretely expressed in the PE and EE [20,21] and regulates the specification and maturation of the proepicardial cells [22] in *Xenopus*, while in mice it has been reported to be essential for epicardial derived fibroblast formation [23] and the inhibition of smooth muscle differentiation [24]. Other cardiac transcription factors with pivotal roles in cardiogenesis, including *Gata4*, *Nkx2.5*, *Isl1* and *Pitx2* have been reported during PE/EE formation [25,26], yet their functional contribution is still uncertain, except *Gata4* that is essential for PE formation [27].

For decades, the adult epicardium was considered merely an external cardiac lining with no or limited physiological implications. However, it has become clearly demonstrated that upon injury, the epicardium is reactivated, providing essential cues to regenerate the damaged heart in experimental models such as zebrafish, medaka and mice [28–33]. While the direct epicardial cellular contribution is limited [34], adult thymosin β4 primed epicardial cells can be converted into fully functionally integrated cardiomyocytes after myocardial infarction [35–37], supporting the therapeutic potential of the epicardium to heal the damaged heart [38–41]. Furthermore, EPDCs play determinant roles in distinct cardiac pathological conditions, contributing to an increased fibrous response after myocardial infarction [42] as well as providing cellular substrates for atrial fat deposition [43] that correlates with an enhanced prevalence of arrhythmogenic diseases such atrial fibrillation [44–46].

Over the last decade, we have witnessed the rise of a novel layer of complexity governing gene regulation with the discovery of non-coding RNAs [47,48]. Non-coding RNAs are broadly classified according to their length into small non-coding RNAs (<200 nt) and long non-coding RNAs (>200 nt) [47,48]. microRNAs constitute the most abundantly expressed and widely studied types of RNAs among small non-coding RNAs. microRNAs are 20-24 nucleotides in length molecules that play essential roles controlling post-transcriptional regulation of coding RNAs by base pair complementary binding within the 3´UTRs and promoting mRNA degradation and/or protein translation blockage [47]. On the other hand, long non-coding RNAs displayed a similar biogenesis as coding RNAs but despite their length, no protein coding potential is identified [48]. Several lncRNAs have been reported to exert

 doi:10.20944/preprints202408.0067.v1

pivotal roles during early embryonic development, such as *Fendrr* and *Braveheart* [49,50], but none of them have been identified during epicardial formation. Furthermore, some lncRNAs have been identified to be distinctly expressed in cardiac pathological conditions such as myocardial ischemia, heart failure or arrhythmogenic diseases, respectively [51–54].

Recently, we have identified three distinct lncRNAs, adjacent to the *Wt1*, *Bmp4* and *Fgf8* chicken gene loci, with enhanced expression in the PE as compared to the embryonic myocardium in the developing embryonic chicken heart. These lncRNAs are distinctly regulated by Bmp, Fgf and thymosin β4, providing support of their plausible implication in epicardial cell lineage specification [55]. Within this study, we therefore provided thorough characterization of their tissue and subcellular distribution, their transcriptional regulation, their conservation in mice and their functional characterization. We provide herein evidence that these lncRNAs are widely distributed and transcriptional regulated by cardiac enriched transcription factors. Furthermore, mouse *Gm14014*, but not its chicken homologue *Wt1_76127*, is required for epicardial cell migration.

2. Results

2.1. Tissue Distribution in the Embryonic Chicken

The analyses of gene expression and tissue distribution are important features for understanding the plausible functional roles of lncRNAs because they can provide hints on their cellular function depends on whether they are expressed in a tissue restricted manner or multiple tissues [68]. We therefore have analyzed by RT-qPCR the expression profile of *Wt1_76127*, *Fgf8_57126* and *Bmp4_53170* lncRNAs in distinct embryonic structures of HH24 and HH32 chicken embryos. Our data demonstrate that *Wt1_76127* and *Fgf8_57126* are predominantly expressed in limb buds and eye with residual expression in the heart at HH24 (Figure 1A). On the other hand, *Bmp4_53170* is preferentially expressed in the eye and upper limb buds, with lower expression in the heart and not detectable levels in the lower limb buds (Figure 1A). At HH32, the expression of *Wt1_76127* remains to be highest in the limb buds followed by the body wall, head, eye and liver with minimal expression in the heart, similarly as at HH24 (Figure 1B). *Fgf8_57126* displays a rather similar expression profile as *Wt1_76127* (Figure 1B), while *Bmp4_53170* displayed the highest expression in the body wall and liver, moderate expression in the heart and limb buds and low expression levels in the head, limb buds and eye (Figure 1B). Overall these data demonstrate that *Wt1_76127* and *Fgf8_57126* display similar expression patterns during embryogenesis, in contrast to *Bmp4_53170*, yet all three of them are widely distributed in different tissues during embryogenesis. These data therefore suggest that these lncRNAs might be functional relevant in multiple tissues.

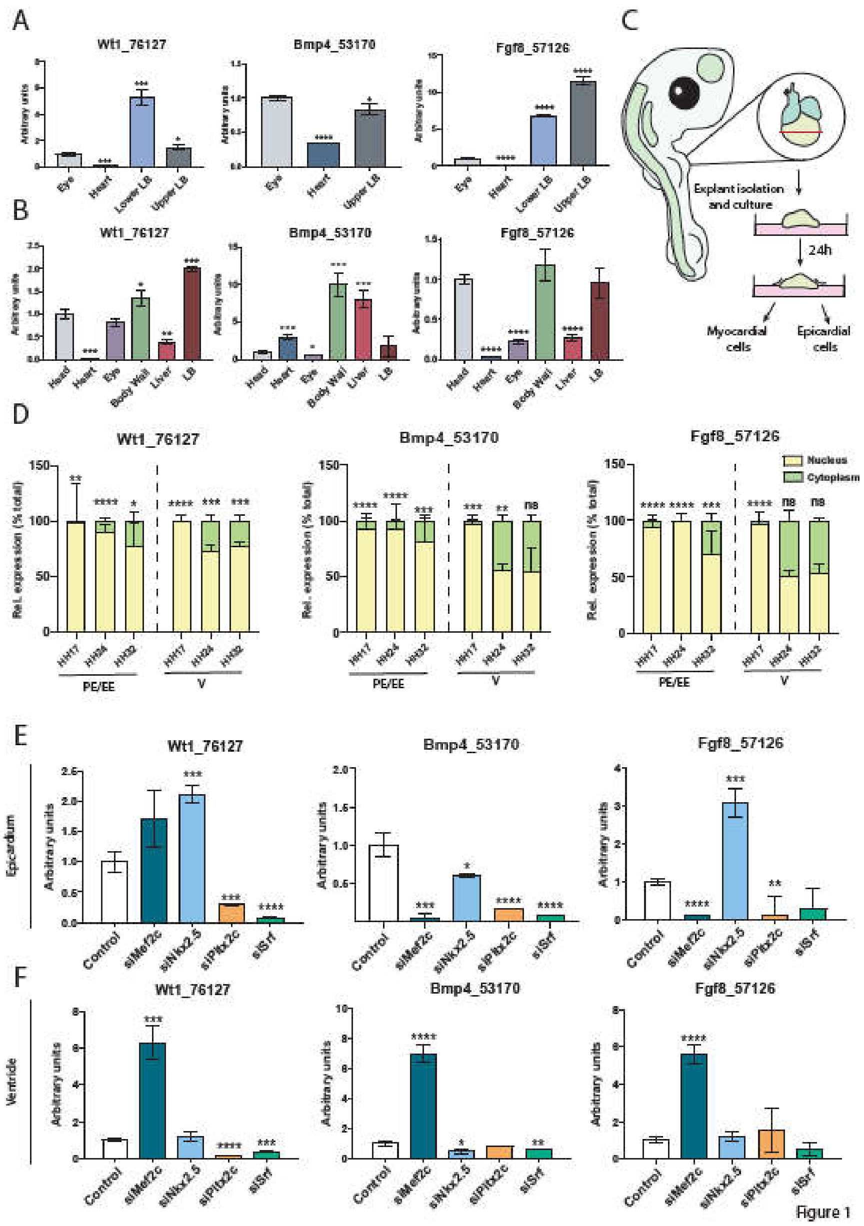

Figure 1. Panel A. RT-qPCR analyses of *Wt1_76127*, *Bmp4_53170* and *Fgf8_57126* in HH24 embryonic tissues, demonstrating a high expression levels in the limb buds as compared to the heart. Panel B. RT-qPCR analyses of *Wt1_76127*, *Bmp4_53170* and *Fgf8_57126* in HH32 embryonic tissues, demonstrating a high expression levels in the limb buds, body wall and liver as compared to the heart and eye. Panel C. Schematic representation of the chicken ventricular explants. Panel D. RT-qPCR analyses of the subcellular nuclear and cytoplasmic distribution of *Wt1_76127*, *Bmp4_53170* and *Fgf8_57126* in HH17, HH24 and HH32 proepicardial (PE; HH17), embryonic epicardial (EE, HH24 and HH32) and ventricular (V, HH17, HH24 and HH32) tissues. Observed that all three lncRNAs are prominently nuclear but their cytoplasmic expression increases as development proceeds, particularly in the ventricular tissues. Panel E. RT-qPCR analyses of *Wt1_76127*, *Bmp4_53170* and *Fgf8_57126* expression in epicardial cells after selective inhibition of *Mef2c*, *Nkx2.5*, *Pitx2c* and *Srf* transcription factors by siRNA administration, respectively. Panel F. RT-qPCR analyses of *Wt1_76127*, *Bmp4_53170* and *Fgf8_57126* expression in ventricular cells after selective inhibition of *Mef2c*, *Nkx2.5*, *Pitx2c* and *Srf* transcription factors by siRNA administration, respectively.

2.2. Subcellular Distribution in Proepicardial, Epicardial and Ventricular Tissues during Development

LncRNAs have been extensively reported to be distinctly located in distinct subcellular compartments; exerting epigenetic and transcriptional roles if preferentially distributed in the nucleus and post-transcriptional roles if in the cytoplasm. We are particularly interested in understanding their functional role in the developing and adult heart, even though the expression of these lncRNAs is low. Therefore, we analyzed their subcellular distribution in the cytoplasmic and nuclear compartments of proepicardial (HH17), epicardial (HH24 and HH32, respectively) and ventricular (HH17, HH24 and HH32, respectively) tissues (Figure 1C). Our data demonstrate that *Wt1_76127*, *Fgf8_57126* and *Bmp4_53170* display a prominent nuclear localization in the proepicardial and epicardial cells at all stages analyzed (Figure 1D). On the other hand, while the expression of *Wt1_76127*, *Fgf8_57126* and *Bmp4_53170* is prominently nuclear at early developmental ventricular stages, *i.e.* HH17, yet they become to be progressively also expressed in the cytoplasm at HH24 and HH32, being almost equally represented for *Fgf8_57126* and *Bmp4_53170*, while *Wt1_76127* remains to be predominantly nuclear (Figure 1D). Thus, these data support the notion that these lncRNAs might preferentially exert epigenetic and transcriptional roles.

2.3. Transcriptional Regulation of Wt1_76127, Fgf8_57126 and Bmp4_53170

Several studies demonstrate the ability of lncRNAs to regulate the expression transcription factors that promote or repress gene expression [69]. However, the expression of lncRNAs is also a transcriptionally regulated process [70], although their transcriptional regulation has been currently scarcely investigated. We sought to investigate whether different cardiac-enriched transcription factors, *i.e. Mef2c*, *Nkx2.5*, *Pitx2c* and *Srf*, can regulate the expression of *Wt1_76127*, *Fgf8_57126* and *Bmp4_53170* lncRNAs in epicardial and ventricular explants. To dissect this point, we performed loss-of-function assays in HH24 epicardial and ventricular explants, respectively, and transfected with their corresponding siRNAs (loss-of-function) as previously reported [62] (Supplementary Figure S1A). Our data demonstrate that silencing *Mef2c* in epicardial explants significantly diminishes the expression of *Bmp4_53170* and *Fgf8_57126* while *Wt1_76127* is not altered (Figure 1E). *Nkx2.5* siRNA administration leads to up-regulation of *Wt1_76127* and *Fgf8_57126* while *Bmp4_53170* expression is down-regulated. On the other hand, silencing *Pitx2c* and *Srf* leads to downregulation of all three lncRNAs (*Wt1_76127*, *Bmp4_53170* and *Fgf8_57126*), except for *Fgf8_57126* that *Srf* siRNA is not significantly altered after *Srf* siRNA administration (Figure 1E). Overall these data suggest that *Mef2c*, *Pitx2c* and *Srf* are essential for transcriptional activation of these three lncRNAs while *Nkx2.5* might be acting as a repressor in the case of *Wt1_76127* and *Fgf8_57126*.

Analyses of loss-of-function assays in ventricular explants also demonstrates a distinct transcriptional regulation by these transcription factors. Silencing *Mef2c* leads to upregulation of all three lncRNAs, *i.e. Wt1_76127*, *Fgf8_57126* and *Bmp4_53170*, in HH24 ventricular explants (Figure 1F). *Nkx2.5* silencing only decreases *Bmp4_53170* while *Wt1_76127* and *Fgf8_57126* are not altered, *Pitx2c* silencing only diminishes *Wt1_76127* but not *Bmp4_53170* or *Fgf8_57126* while *Srf* silencing in ventricular explants only decreases *Bmp4_53170* and *Wt1_76127* but *Fgf8_57126* is not modified (Figure 1F). Thus, these data suggest that *Mef2c* plays a fundamental role repressing the expression of all three lncRNAs in the ventricular explants while the role of the other three cardiac-enriched transcription factors is spurious and limited to *Wt1_76127* and *Bmp4_53170*, respectively.

Since we have previously observed that these lncRNAs display a dynamic subcellular distribution during embryonic development, we sought to investigate if silencing these transcription factors might distinctly regulate the subcellular distribution in the embryonic epicardium, focusing particularly on *Mef2c*. Loss-of-function of *Mef2c* in epicardial explants in HH24 did not modify nuclear *vs* cytoplasmic distribution of *Wt1_76127*, enhanced *Bmp4_53170* expression in both subcellular compartments and selectively down-regulated *Fgf8_57126* expression in the nucleus while not altering cytoplasmic expression (Supplementary Figure S1B). Nuclear *vs* cytoplasmic distribution in *Fgf8_57126* in HH32 remained the same as in HH24 after loss-of- function of *Mef2c*, although it negatively regulated *Wt1_76127* nuclear distribution and *Bmp4_53170* cytoplasmic distribution, respectively (Supplementary Figure S1C). Thus, these data support the notion that cytoplasmic *vs* nuclear localization is modulated in part by *Mef2c*.

2.4. Wt1_76127 Is Conserved in the Mouse (Gm14014)

Conservation of lncRNAs in different species is currently rarely identified as lncRNAs seem to be less conserved than coding-RNAs. [48,71]. We sought to investigate if *Wt1_76127*, *Fgf8_57126* and *Bmp4_53170* are conserved in the mouse genome. Analyses of the lncRNAs annotated in the mouse genome lead to the identification of *Gm14014* as a putative homologue of *Wt1_76127*, since it is located in the vicinity of the Wt1 locus and it shares a 39,1% homology identity with *Wt1_76127* (Supplementary Table S2). Comparative analyses of such nucleotide conservation display a wide and heterogeneous distribution of such conserved nucleotide stretches in *Gm14014* (Supplementary Figure S2). On the other hand, no homologues for *Fgf8_57126* and *Bmp4_53170* were found.

2.5. Gm14014 Is Widely Expressed in Mouse Embryonic Tissues

To investigate whether the homology between *Wt1_76127* and *Gm14014* correlates with similar expression patterns and determine if *Gm14014* is a lncRNA with ubiquitous expression (as *Wt1_76127*) or is a tissue-specific lncRNA, we tested *Gm14014* expression in multiple tissues during embryonic development. RT-qPCR analyses demonstrated that in mouse E13.5 embryos *Gm14014* is more abundantly expressed in the lungs, stomach, kidney and liver as compared to the head, while similar expression levels are observed in the intestine and lower expression levels are detected in the heart (Figure 2A). Analyses of *Gm14014* by RT-qPCR in adult mice also displayed a wide tissue distribution. The lungs, stomach and intestine displayed the highest expression levels as compared to the brain, followed by the left and right atria, liver, skeletal muscle, kidney and ventricle (Figure 2B). Overall these data are in line with those observed for *Wt1_76127* in chicken embryos, displaying a wide tissue distribution and low expression levels in the developing heart.

To get further insights into the tissue distribution of *Gm14014*, single molecule SCRINSHOT analyses were performed in embryonic (E14.5) and postnatal (P21) hearts. *Gm14014* SCRINSHOT analyses showed a similar tissue distribution at both stages (Figure 2C,D), indicating the specific position of Gm14014-positive cells (Supplementary Figure S3C). Subsequently, colocalization analyses with muscular (*Acta2*) [72], epicardial (*Col1a2*) [73] and fibroblast (*Sox9*) [74] markers were performed (Figure 2E). The highest colocalization was identified between *Gm14014* and *Sox9* (5.11 %) in E14.5, while in P21 it was significantly decreased (0.03%). *Gm14014* colocalization with *Col1a2* and *Acta2* in E14.5 was 3.62% and 2.87% respectively, while in P21 it was 0.14% in both cases. Furthermore, the global *Gm14014* signal quantification was higher in E14.5 than in P21 (Supplementary Figure S3D). These data demonstrate therefore that *Gm14014* is widely distributed in different cell types in the embryonic and adult heart, displaying higher expression in embryonic stages.

Preprints.org (www.preprints.org) | NOT PEER-REVIEWED | Posted: 2 August 2024 doi:10.20944/preprints202408.0067.v1

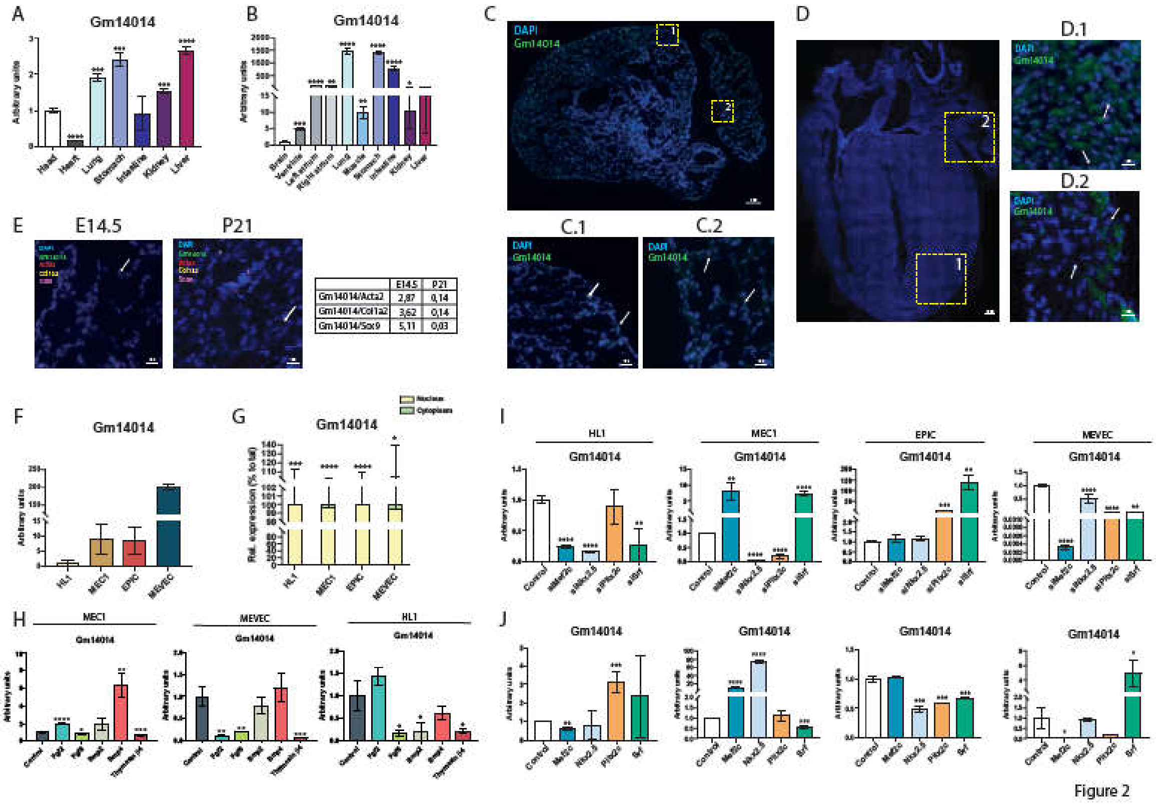

Figure 2. Panel A. RT-qPCR analyses of *Gm14014* expression in embryonic (E13.5) mouse tissues, demonstrating wide expression in different tissues, being higher in the lung, stomach and liver as compared to other tissues, *e.g.* heart. Panel B. RT-qPCR analyses of *Gm14014* expression in adult (3 months old) mouse tissues, demonstrating wide expression in different tissues, being higher in the lung, stomach and liver as compared to other tissues, *e.g.* heart. Panel C. SCRINSHOT *in situ* hybridization analyses of *Gm14014* expression in E14.5 mouse hearts, panel C.1 and C.2 are close ups corresponding to atrial and ventricular areas, respectively. Panel D. SCRINSHOT *in situ* hybridization analyses of *Gm14014* expression in 21 days postnatal (P21) mouse hearts, panel D.1 and D.2 are close ups corresponding to atrial and ventricular areas, respectively. Panel E. SCRINSHOT *in situ* hybridization analyses of *Gm14014*, *Acta2*, *Col1a2* and *Sox9* expression colocalization in E14.5 and P21 mouse hearts, corresponding to ventricular closeups, respectively. Panel F. RT-qPCR analyses of *Gm14014* expression in HL1 cardiomyocytes, MEC1 and EPIC epicardial cells, and MEVEC endocardial cells. Observe higher expression levels in MEVEC endocardial cells as compared to MEC1 and EPIC epicardial cells, with lower expression levels in HL1 cardiomyocytes. Panel G. RT-qPCR analyses of the subcellular nuclear and cytoplasmic distribution of *Gm14014* in HL1 cardiomyocytes, MEC1 and EPIC epicardial cells, and MEVEC endocardial cells. Note that in all cases, *Gm14014* is prominently nuclear. Panel H. RT-qPCR analyses of *Gm14014* expression in MEC1 epicardial cells, MEVEC endocardial cells and HL1 cardiomyocytes after selective administration of *Fgf2*, *Fgf8*, *Bmp2*, *Bmp4* and thymosin β4, respectively. Panel I. RT-qPCR analyses of *Gm14014* expression in HL1 cardiomyocytes, MEC1 and EPIC epicardial cells, and MEVEC endocardial cells after selective inhibition of *Mef2c*, *Nkx2.5*, *Pitx2c* and *Srf* transcription factors by siRNA administration, respectively. Panel J. RT-qPCR analyses of *Gm14014* expression in HL1 cardiomyocytes, MEC1 and EPIC epicardial cells, and MEVEC endocardial cells after selective overexpression of *Mef2c*, *Nkx2.5*, *Pitx2c* and *Srf* transcription factors, respectively.

2.6. Gm14014 Is Nuclearly Located and Displays Tissue-Specific Transcriptional Regulation

In order to further characterize the cardiovascular expression of *Gm14014* and thus to determine its plausible biological role in this context, we analyzed the expression of *Gm14014* in different cardiac cell lines, as well as its subcellular localization. Moreover, since regulation of lncRNA expression is similar to that of coding RNAs, we investigated the impact of growth factors and key transcription factors involved in cardiogenesis in *Gm14014* expression. We analyzed *Gm14014* expression level in four distinct cardiac cell lines, *i.e.* HL1 atrial cardiomyocytes, MEC1 and EPIC epicardial cells and MEVEC endocardial cells. Our data demonstrate that the highest expression is observed in endocardial MEVEC cells, followed by EPIC and MEC1 epicardial cells, with the lowest expression in HL1 atrial cardiomyocytes (Figure 2F). Importantly, subcellular localization analyses by RT-qPCR, demonstrated that *Gm14014* is primarily located in the nucleus in all four distinct cell lines (Figure 2G & Supplementary Figure S3A).

It has been previously demonstrated that several members of the Fgf and Bmp families, e.g. *Bmp2*, *Bmp4*, *Fgf2* and *Fgf8*, are essential players of cell fate determination during cardiogenesis, particularly during PE/EE development [10,75]. We have also recently demonstrated that *Wt1_76127*, *Fgf8_57126* and *Bmp4_53170* are distinctly regulated by these growth factors as well as by thymosin β4. We therefore scrutinize herein whether these growth factors are able to modulate *Gm14104* in the different cardiac cell lines. Within epicardial (MEC1) cells, *Gm14014* expression is increased after *Fgf2* and *Bmp4* administration, respectively, while addition of *Bmp2* displayed no significant differences and *Fgf8* as well as thymosin β4 significantly down-regulated it (Figure 2H). Additionally, we also tested if these growth factors could also influence *Gm14014* in MEVEC endocardial and HL1 cardiomyocytes. In endocardial MEVEC cells, *Fgf2*, *Fgf8* and thymosin β4 administration resulted in significant *Gm14014* downregulation while *Bmp2* and *Bmp4* lead to no significant differences (Figure 2H). Within HL1 cells, *Fgf8*, *Bmp2* and thymosin β4 administration significantly down-regulate *Gm14014* expression, while *Fgf2* and *Bmp4* resulted in no significant differences (Figure 2H). Therefore, these data demonstrate that both Fgfs and Bmps can distinctly modulate *Gm14014* in different cell types. Curiously, thymosin β4 administration consistently downregulated *Gm14014* in all three cardiovascular cell types.

We subsequently tested the functional role of distinct cardiac enriched transcription factors in these four different cell lines using gain- and loss-of-function assays for *Mef2c*, *Nkx2.5*, *Pitx2c* and *Srf* transcription factors (Supplementary Figure S3B). Within HL1 atrial cardiomyocytes, *Gm14014* is significantly down-regulated by *Nkx2.5* and *Srf* inhibition while over-expression of these transcription factors did not significantly modulate its expression (Figure 2I,J). On the other hand, *Pitx2c* over-expression, but not inhibition, significantly upregulated *Gm14014* (Figure 2I,J). Curiously, both *Mef2c* gain- and loss-of-function assays led to significant downregulation of *Gm14014* in this cell type (Figure 2I,J). Overall, these data demonstrate that *Mef2c*, *Nkx2.5* and *Srf* are indispensable for *Gm14014* expression while *Pitx2c* on its own is capable to enhance *Gm14014* expression in cardiomyocytes.

Gm14104 expression in MEC1 epicardial cells is equally upregulated by *Mef2c* gain and loss-of-function, while *Nkx2.5* inhibition significantly down-regulated and *Nkx2.5* over-expression upregulated *Gm14014* (Figure 2I,J). In contrast, *Srf* inhibition significantly up-regulates, while *Srf* over-expression downregulates *Gm14014*, displaying therefore opposite regulatory capabilities to *Nkx2.5* (Figure 2I,J). On the other hand, only *Pitx2c* inhibition selectively down-regulates *Gm14014* while *Pitx2c* over-expression does not modulate its expression (Figure 2I,J). Therefore, these data demonstrate that *Nkx2.5* and *Srf* play fundamental and opposite roles regulating *Gm14014* in MEC1 epicardial cells, while only *Pitx2c* silencing modulates its expression.

Within EPIC epicardial cells, the modulatory roles of these transcription factors seem to be substantially different as for MEC1 epicardial cells, probably correlating with the epicardial nature of MEC1 as compared to EPIC that display mixed epicardial and mesenchymal behavior. *Mef2c* and *Nkx2.5* silencing does not modulate *Gm14014* while *Pitx2c* and *Srf* inhibition significantly up-regulates its expression (Figure 2I,J). On the other hand, *Mef2c* over-expression does not modulate *Gm14014* while *Nkx2.5*, *Pitx2c* and *Srf* significantly down-regulated *Gm14014*, respectively (Figure 2I,J). Therefore, *Pitx2c* and *Srf* are essential factors for *Gm14014* expression in EPIC cells and only *Srf* displays similar regulatory effects in MEC1 and EPIC cells.

Finally within MEVEC endocardial cells, *Mef2c* inhibition and over-expression significantly down-regulated *Gm14014* expression (Figure 2I,J), while *Nkx2.5* and *Pitx2c* inhibition significantly downregulated Gm140*14*, while their over-expression did not significantly alter its expression (Figure 2I,J). On the other hand, *Srf* inhibition downregulated while *Srf* over-expression upregulated *Gm14014* in MEVEC endocardial cells (Figure 2I,J). Therefore, all four transcription factors analyzed are

Preprints.org (www.preprints.org) | NOT PEER-REVIEWED | Posted: 2 August 2024 doi:10.20944/preprints202408.0067.v1

essential for *Gm14014* expression in MEVEC endocardial cells, yet only *Srf* overexpression is capable of inducing *Gm14014* expression. Consequently, these data demonstrate that expression of *Gm14014* is regulated in part by *Mef2c*, *Nkx2.5* and *Srf* in HL1 cardiomyocytes, *Nkx2.5* and *Pitx2c* in MEC1 epicardial cells and *Mef2c*, *Nkx2.5*, *Pitx2c* and *Srf* in MEVEC endocardial cells but is not critically dependent on any of the tested transcription factors in EPIC cells, as revealed by the siRNA assays.

2.7. Gm14014 Is Distinctly Regulated upon Myocardial Injury

Epicardial activation has been reported to be induced after myocardial injury [76–81], significantly contributing to myocardial regeneration. We therefore established an *ex vivo* model to dissect if *Gm14014* is activated after cryoinjury and thus might be involved in regeneration. Ventricular explants for mouse E10.5, E13.5, E19.5 and postnatal day (P1) hearts were cultured and cryoinjured with a liquid nitrogen freeze needle and incubated at different times, ranging from 6-48 hours post-injury (Figure 3A). *Gm14014* displayed increasing expression levels after cryoinjury ranging from 6 to 48 hours post-injury in E10.5, E13.5 (except at 48h) and E19.5 ventricular explants while it decreases at 24h and 48h in P1 cryoinjured ventricular explants (Figure 3B).

In the regeneration context, it has been shown that the timing of injury is crucial in achieving cardiac regeneration. Cardiac damage at P1 stage allows almost complete regeneration after one month, whereas at P7 such ability is largely reduced [82]. Therefore, we tested whether cryoinjury modulates the expression of *Gm14014* as well as distinct molecular markers related to epicardial activation (*Wt1*, *Tbx18*, *Tcf21*), epithelial to mesenchymal transition (*Snail1*, *Snail2*, *Cdh5*) and cardiomyogenic maturation (*Tnnt2*) at 24h post-injury in ventricular explant for mouse E10.5, E13.5, E19.5, P1 and P7 stage. Epicardial activation markers (*Wt1*, *Tbx18* and *Tcf21*) are barely modulated in cryoinjured embryonic stages while they are significantly upregulated at P1 cryoinjured hearts and considerably decreased at P7 (Figure 3C and Supplementary Figure S4). Importantly, *Tcf21* is also significantly upregulated at E19.5 (Figure 3C and Supplementary Figure S4). These data therefore suggest that epicardial activation is exclusively observed at P1 concomitantly with *Gm14014* down-regulation, while at P7 the epicardial activation is significantly reduced and *Gm14014* is increased, showing a complementary patterns between P1 and P7 stages. We subsequently analyzed epithelial to mesenchymal transition markers such as *Snail1*, *Snail2* and *Cdh5*, and cardiomyogenic maturation makers such as *Tnnt2* (Figure 3C and Supplementary Figure S4). These markers display a similarly overt expression profile upon cryoinjury, *i.e.* no modulation or down-regulation at embryonic stages, up-regulation at P1 and a down-regulation in P7 cryoinjured hearts, further reinforcing the inverse correlation between *Gm14014* modulation upon cryoinjury and the activation of these molecular markers. Furthermore, these data support the notion that *Gm14014* might be relevant during cardiac regeneration, given its differential regulation in neonatal stages with regenerative (P1) vs non regenerative (P7) potential.

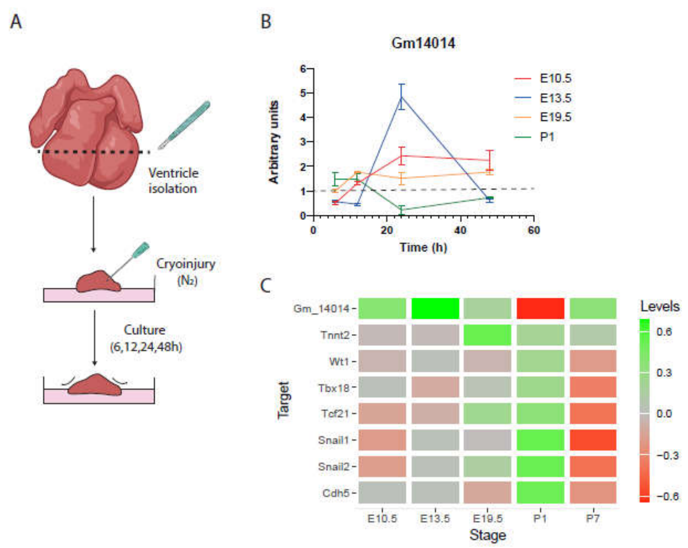

Preprints.org (www.preprints.org) | NOT PEER-REVIEWED | Posted: 2 August 2024 doi:10.20944/preprints202408.0067.v1

Figure 3. Panel A. Schematic representation of the mouse ventricular explants for *ex vivo* cryoinjury. Panel B. RT-qPCR analyses of *Gm14014* expression in E10.5, E13.5, E19.5 and P1 mouse ventricular explant at 6h, 12h, 24h and 48h after cryoinjury, respectively. Observe that *Gm14014* progressively increases over time at embryonic stages while it decreases at postnatal stage. Panel C. Heatmap representation of the expression levels of myocardial (*Tnnt2*), epicardial (*Wt1, Tbx18, Tcf21*) and EMT (*Snail1, Snail2, Cdh5*) markers in E10.5, E13.5, E19.5, P1 and P7 mouse ventricular explants at 24h after cryoinjury, respectively.

2.8. Identification of Gm14014 Interacting Proteins

LncRNAs can exert their function interactive with different types of molecules, including other RNAs species and protein. Importantly, dissenting lncRNA-protein interactions can provide hints of their roles in post-transcriptional regulation [83,84]. In order to get further insights into the molecular mechanisms driven by lncRNA *Gm14014* in epicardial context, we performed RNA pull-down (PD) assays followed by mass spectrometry (MS) to identify *Gm14014* associated proteins in epicardial MEC1 cells. A total of 315 proteins were uniquely identified in the *Gm14014* PD assays as compared to input and *Gapdh* PD controls (Supplementary Table S3); ~25% were exclusively nuclear, ~30% were exclusively cytoplasmic and ~28% were present in both compartments (Supplementary Table S3). Gene ontology (GO) analyses of uniquely identified proteins in *Gm141014* PD where primarily involved in biological processes such as mRNA processing, translation, mRNA processing RNA splicing, protein transport, positive regulation of gene expression, cytoplasmic translation, RNA splicing-via spliceosome and actin cytoskeleton organization (Supplementary Figure S5A). These results highlight the prominent role of *Gm14014* in association with nuclear biological processes, in line with its predominant nuclear localization, although it is importantly to detail that distinct cytoplasmic biological functions are also identified.

GO analyses of cellular components revealed that cytoplasm, cytosol, nucleus, nucleoplasm, cytoskeleton synapse and nucleolus as the most representative compartments (Supplementary Figure S5B). Finally, GO molecular function analysis identified protein binding, nucleotide binding, RNA binding, identical protein binding, nucleic acid binding, ATP binding and actin binding as the most represented functions (Supplementary Figure S5C). Thus, all GO analyses support a dual nuclear and cytoplasmic role for *Gm14014*.

We subsequently focused our attention on those cellular compartments and molecular and biological functions with a higher number of uniquely identified proteins in *Gm14014* PD, *i.e.* cytoplasm, protein binding and translation. Among these categories, several families of proteins are highly represented, such as ribosylation factors, DEAD box helicases, small GTPases RAB proteins, splicing factors, ribosomal proteins and cytoskeletal proteins. Additionally, multiple cytoskeletal proteins were found to interact with *Gm14014*, including those controlling actin filament organization (Rac1), positive and negative action polymerization (cofilin, profilin, gelsolin, filamin) and actin interacting proteins (actins, actinins, myosins, talin, tubulin, tropomyosin and vinculin). These findings suggest therefore that *Gm14014* might be involved in cytoskeletal organization, plausible playing a role in cell cytoskeletal remodeling and/or migration.

2.9. Dissecting the Functional Role of Gm14014 in Epicardial Cell Migration

As mentioned above, epicardial cell migration is a critical process during embryonic development, allowing the external coverage the myocardium as well as promoting epicardial derived cells to invade the myocardium. Importantly, epicardial cell migration is not only required during embryogenesis, but also after cardiac injury when epicardial cells are activated to promote cardiac regeneration. To elucidate a plausible role for *Gm14014* in the epicardial cell migration process, we performed a loss-of-function assay of *Gm14014* in MEC1 epicardial cell line. We designed two distinct ASOs and demonstrated that ASO1, but not ASO2, was capable of inhibiting *Gm14014* expression (Supplementary Figure S6A) after 6 hours of transfection. Thereafter we tested the timeframe of *Gm14014* ASO1 inhibition demonstrating that consistent downregulation was also observed at 12h and 18h while at 24 hours, inhibition was blunted and an overt upregulation was

 doi:10.20944/preprints202408.0067.v1

promoted (Figure 4A). Surprisingly, 48h after transfection, downregulation was detected again (Figure 4A). Based on these results, all *Gm14014* inhibitions were carried out only with ASO1 (*i.e.* ASO from now on).

To determine the effect of *Gm14014* inhibition on the migration process, we carried out cell migration assays, which were performed by generating a scratch into the semi-confluent MEC1 epicardial cells and monitored for 24 hours in controls and *Gm14014* ASO treated conditions. Analyses of the migratory cells demonstrated that *Gm14014* ASO treated cells were consistently delayed at 8, 12 and 24 hours, demonstrating a functional role for *Gm14014* in epicardial cell migration (Figure 4B). Furthermore, phospho-histone 3 (pHH3) immunohistochemical assays demonstrate no significant differences in cell proliferation, supporting the notion that such migratory differences are independent of cell proliferation (Figure 4C). In addition, time-lapse analyses demonstrated that *Gm14014* inhibition lead to impaired cell migration as compared to controls, provided that non-linear migration (*i.e.* random) was significantly increased (Figure 4D and Supplementary Figure S6B).

To uncover if the functional role of *Gm14014* in migration also occurs in other cardiovascular cell types, scratch assays were also performed in HL1 cardiomyocytes and MEVEC endocardial cells. Importantly, no differences in cell migration were observed at any time point analyses (Figure 4B), supporting the notion that *Gm14014* role in cell migration is cell type specific, *i.e.* epicardial cells.

Multiple cytoskeletal proteins were identified in our PD assay to interact with *Gm14014*, including those controlling actin filament organization (Rac1), positive and negative action polymerization (cofilin, profilin, gelsolin, filamin,) and acting interacting proteins (actins, actinins, talin, tubulin, myosins, tropomyosin and vinculin). We therefore tested whether differences in epicardial cell migration after *Gm14014* inhibition are induced by changes in the cell cytoskeleton. Immunocytochemical analyses of Actn1, Actn4 and Rac1 displayed no significant differences between *Gm14014* ASO treated epicardial cells and controls at 6h (*Gm14014* downregulated) or 24h (*Gm14014* upregulated) (Figure 4E). On the other hand, Myh9 and Myl9 displayed significant differences at 6h after ASO administration, since *Gm14014* inhibition significantly reduced Myl9 and Myh9 protein levels. However, when *Gm14014* is upregulated at 24h after ASO treatment, we only observed increased Myh9 protein levels, while for Myl9 there are no significant differences (Figure 4E). Furthermore, no differences in the expression of Myh9 and Myl9 were observed in HL1 atrial cardiomyocytes at both 6 and 24h, in line with their lack of migration differences following *Gm14014* ASO1 administration (Supplementary Figure S6D,E). It is importantly to highlight in this context that Myl9 expression is significantly diminished in both nuclear and cytoplasmic compartments while Myh9 only displayed differences at cytoplasmic level (Figure 4E). Such observations might be linked to the capacity of Myl9 to translocate into the nucleus and exert transcriptional activity [85,86]. To further sustain the plausible role of *Gm14014* modulating such cytoskeletal proteins, PD assays and WB were performed, confirming that Myl9, but not Rac1, interacted with *Gm14014* (Figure 4F). To support the possible role of *Gm14014* regulating epicardial cell migration through cytoskeletal protein binding, *Myl9* loss-of-function assay were performed. Two different strategies were employed: *Myl9* siRNA to inhibit its expression in the cytoplasm, and *Myl9* ASO to inhibit its expression, both in the nucleus and cytoplasm (Supplementary Figure S6C). These results were similar to those obtained with *Gm14014* inhibition, showing a reduction in epicardial cell migration capacity from 6h to 24h when *Myl9* expression levels are diminished at both cellular compartments (Figure 4B). Thus, these data demonstrate the involvement of *Gm14014* in modulating cytoskeletal proteins that play a regulatory role in the epicardial cell migration process.

Preprints.org (www.preprints.org) | NOT PEER-REVIEWED | Posted: 2 August 2024 doi:10.20944/preprints202408.0067.v1

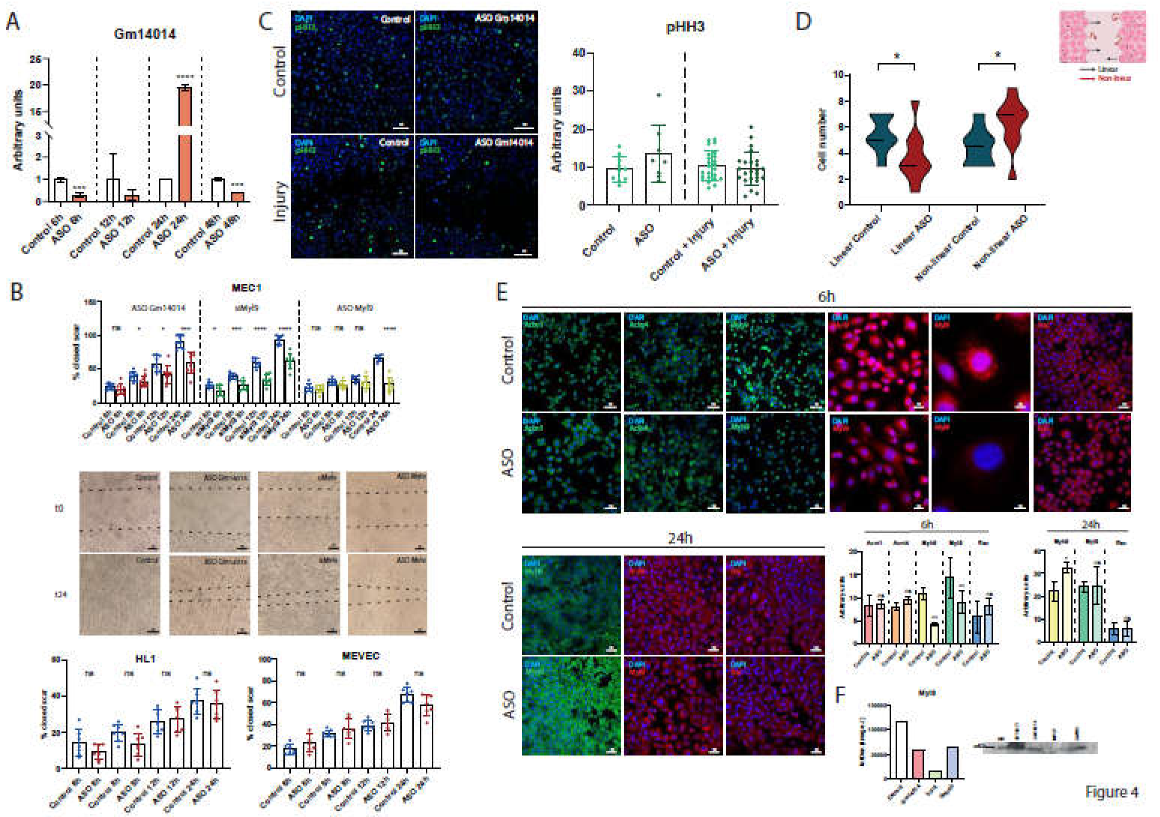

Figure 4. Panel A. RT-qPCR analyses of *Gm14014* expression in MEC1 epicardial cells after *Gm14014* ASO administration at 6h, 12h, 24h and 48h after transfection. Observe that selective downregulation is achieved at 6h,12h and 48h while at 24h there is a significant upregulation. Panel B. Schematic representation of wound healing scratch assay in MEC1 epicardial cells in controls, *Gm14014* ASO, siMyl9 and *Myl9* ASO treated cells, respectively, HL1 cardiomyocytes and MEVEC endocardial cells at 6h, 8h, 12h and 24h in controls and *Gm14014* ASO treated cells, respectively. Representative images at t=0 and t=24h in MEC1 epicardial cells. Note that *Gm14014* ASO treated cells are significantly decreased in migration in MEC1 epicardial cells but not in HL1 cardiomyocytes and MEVEC endocardial cells. siMyl9 and *Myl9* ASO treated cells are significantly decreased in migration in MEC1 epicardial cells. Panel C. Representative images of proliferation assays as revealed by phospho-histone 3 (pHH3) immunocytochemistry in control and scratched MEC1 epicardial cells corresponding to control and *Gm14014* ASO conditions. Quantitative analyses are also shown demonstrating no significant differences in cell proliferation. Panel D. Graphical representation of lineal vs non-lineal cell migration in time-lapse confocal image analyses of control and scratched MEC1 epicardial cells corresponding to control and *Gm14014* ASO conditions. Panel E. Representative images of immunocytochemical analyses of Actn1, Actn4, Myh9, Myl9, Rac1 at 6h and of Myh9, Myl9, Rac1 at 24h after administration of *Gm14014* ASO as compared to controls. Observe that there is significant difference in the expression of Myh9 and Myl9 at 6h but not at 24h. Note also that Myl9 displays both nuclear and cytoplasmic distribution in controls while in *Gm14014* treated cell is exclusively cytoplasmic. Panel F. Quantitative analysis and representative blot of Myl9 after *Gm14014* PD. Observe that Myl9 protein interacts with Gm14014.

2.10. Dissecting the Functional Role of Wt1_76127

Gm14014 displayed almost 40% nucleotide similarity to *Wt1_76127* (Supplementary Table S2). However, it remains unclear if such limited sequence conservation is sufficient to maintain similar molecular functional capabilities. In other to get insights into the plausible conserved functional role of *Wt1_76127*, we designed an ASO against this lncRNA since it is predominantly nuclear. We isolated primary cultures of cardiac embryonic fibroblasts and cardiomyocytes as a proxy to test the plausible functional role of *Wt1_76127*. Expression of *Wt1_76127* was primarily detected in cardiomyocytes (Figure 5A), particularly in the nucleus (Figure 5B) and therefore we selected this cell type for further analyses. Inhibition with 20nM *Wt1_76127* ASO yielded almost 70-80% of inhibition in both cardiomyocytes and epicardial cells (Figure 5C). Cell viability was assayed in CMs, demonstrating that no differences after *Wt1_76127* inhibition, while a small but significant increase in apoptosis was detected (Figure 5D).

To analyze the possible functional conservation between *Gm14014* and *Wt1_76127*, proliferation and migration in CMs were analyzed after ASO treatment, displaying no significant no differences in both cases (Figure 5E–G). Curiously, cytoskeletal protein such as Actn1 and Myh9, but not Actn4 were significantly downregulated (Figure 5J). Additional experiments using epicardial explants assays demonstrated neither significant differences in cell migration (Figure 5H) nor in Actn1, Actn4 or Myh9 immunohistochemical detection in migrating epicardial cells (Figure 5I). Therefore, these data demonstrated that *Wt1_76127* inhibition does not influence epicardial and/or myocardial cell migration in chicken embryos and suggest that the function of this lncRNA is not conserved across species.

To further explore the plausible role of *Wt1_76127* during embryonic development, *in vivo* pericardial injections were performed in HH17 chicken embryos (Supplementary Figure S7A). Viability was not compromised by intrapericardial injections of Wt1_76127 ASO (Supplementary Figure S7B). Similarly, cardiac rhythm, i.e. beats per minutes and beating regularity, and cardiac development were neither compromised (Supplementary Figure S7C,D). To further confirm the in vitro data obtained by Wt1_76127 silencing, we isolated and ex vivo cultured ventricular explants after ASO administration and the migration capacity of epicardial cells was analyzed. No significant differences in epicardial cell migration between control and ASO-treated explants was observed (Supplementary Figure S7E), supporting the notion that the function of *Wt1_76127* and *Gm14014* lncRNAs is not conserved between species.

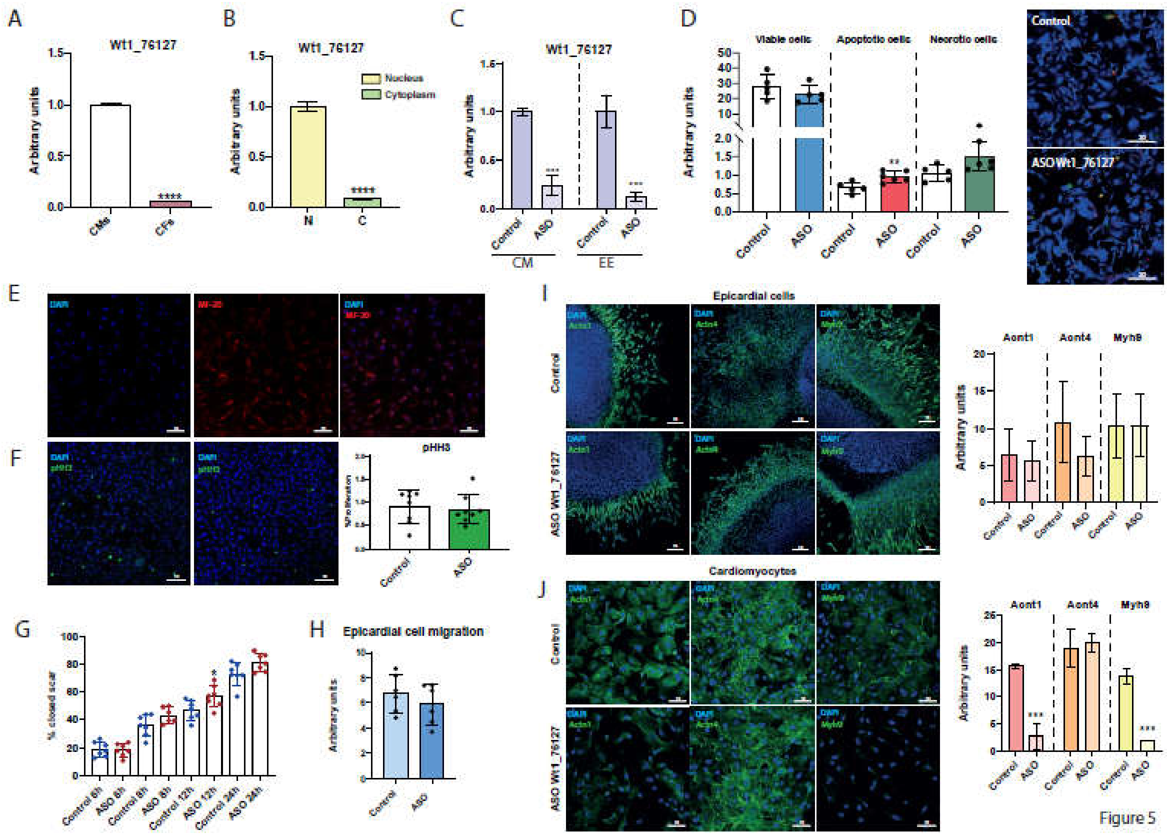

Figure 5. Panel A. RT-qPCR expression analyses of *Wt1_76127* in primary cultures of chicken embryonic cardiomyocytes (CMs) and cardiac fibroblasts (CFs). Panel B. Subcellular distribution of *Wt1_76127* in the nucleus and cytoplasm primary cultures of chicken embryonic cardiomyocytes. Panel C. RT-qPCR expression analyses of *Wt1_76127* in embryonic cardiomyocytes and embryonic epicardium (EE) in control and *Wt1_76127* ASO treated conditions. Observe a significant downregulation in *Wt1_76127* after ASO administration. Panel D. Quantitative analyses of cell

Preprints.org (www.preprints.org) | NOT PEER-REVIEWED | Posted: 2 August 2024 doi:10.20944/preprints202408.0067.v1

viability, apoptosis and necrosis in primary cultures of chicken embryonic cardiomyocytes (CMs) of control and *Wt1_76127* ASO treated conditions. Representative images are also depicted. Note not significant differences for cell viability and necrosis, whereas there are significant differences in apoptosis. Panel E Immunocytochemical characterization of primary culture of embryonic cardiomyocytes with MF20 antibody, demonstrating that most of these cell display sarcomeric myosins. Panel F. Immunocytochemical characterization of proliferation in scratched primary culture of embryonic cardiomyocytes. Observe that there are no significant differences. Panel G. Schematic representation of wound healing scratch assay in primary culture of embryonic cardiomyocytes at 6h, 8h, 12h and 24h in controls and *Wt1_76127* ASO treated cells, respectively. Panel H. Quantitative analyses of epicardial cell migration in ventricular explant in control and *Wt1_76127* ASO treated conditions. Observe that there are no significant differences. Panel I. Representative images of ventricular explants immunostained against Actn1, Actn4 and Myh9 in control and *Wt1_76127* ASO treated conditions. Observe that there are no significant differences. Panel J. Representative images of primary culture of embryonic cardiomyocytes immunostained against Actn1, Actn4 and Myh9 in control and *Wt1_76127* ASO treated conditions. Observe that and Myh9, but not Actn4 display significant differences.

3. Discussion

LncRNAs represent a large family of non-coding RNAs with a wide cellular and tissue distribution. We have previously characterized three newly identified lncRNAs in the chicken genome that display enhanced expression in the developing PE as compared to the embryonic ventricle [55]. We now further elaborated into distinct characteristics of these lncRNAs, including a more detailed analysis of their tissue distribution, transcriptional regulation, functional role and evolutionary conservation in mice. Our data demonstrated that these lncRNAs displayed a broad tissue distribution, in line with other reports demonstrating a global expression of lncRNAs in different tissues [87–89]. In addition, we also demonstrated that these lncRNAs are preferentially nuclearly located, supporting in first instance a more plausible role in transcriptional and/or epigenetic regulation [68]. Intriguingly, their subcellular localization is modulated as embryonic development advances in a tissue-specific manner, i.e. more prominent in the embryonic ventricles as compared to the PE/EE. Thus, these observations support the notion of a dynamic lncRNA subcellular localization that might reflect changes in their maturation and/or biological function [90], a process that seems to be distinctly regulated by transcription factors such as *Mef2c*, as demonstrated herein.

Cardiac-enriched transcription factors such as *Mef2c* [91–93], *Nkx2.5* [94–96] *Srf* [97,98] and *Pitx2* [99–102] play pivotal roles in cardiogenesis as well as in proepicardial/embryonic epicardial development [103–106] by transcriptionally regulating multiple downstream targets, particularly in heart development. While ample evidence is reported on transcriptional regulation of protein-coding RNA [107–110], scarce evidence is available regarding non-coding RNAs, particularly lncRNAs [62,111,112]. We provide herein evidence that *Mef2c* exerts a robust transcriptional repression in embryonic ventricle but not in the epicardium (except for *Wt1_76127*) while such repressive signals are mostly mediated by *Nkx2.5* in the epicardium. On the other hand, *Pitx2c* and *Srf* are essential for proper lncRNAs expression in the epicardium while mostly dispensable in the embryonic ventricle. Overall these data reinforce the notion that lncRNA transcriptional expression is modulated by distinct cardiac-enriched transcription factors, as previously reported for other lncRNAs [62,111] in a tissue-specific manner.

Long non-coding RNAs are poorly conserved non-coding RNA molecules [48,71], in contrast to microRNAs [47]. We could only identify a mouse homologue for *Wt1_76127* in the mouse genome, given that is located in the syntenic genomic locus, *i.e.* the vicinity of *Wt1* transcription factor and shares a 39,1% nucleotide homology. Analyses of its embryonic and adult tissue distribution as well as its subcellular distribution within distinct cardiovascular cellular types display a rather similar profile as its chicken homologue, further supporting its evolutionary conservation.

On the other hand, transcriptional regulation of *Gm14014* displays a mixture of similar control mechanisms as the chicken *Wt1_76127* homologue, as *Nkx2.5* and *Srf* are completely dispensable for their expression in myocardial cells while *Mef2c* and *Pitx2c* exert repressive and activation capacities on epicardial cells. On the other hand, divergent roles for *Mef2c* and *Pitx2c* are observed in myocardial cells, displaying opposite transcriptional regulation in chicken vs mouse. Thus, these data support the notion that cardiac-enriched transcription factors can distinctly and selectively regulate homologue lncRNA expression in a cell-specific manner, as previously reported for other lncRNAs [62,111,113]. Furthermore, transcriptional regulation of lncRNAs seems to rapidly evolved among different species, as previously reported [48,71], supporting the notion that they might even exert divergent functional roles in chicken *vs* mice.

Cardiac injury, such as myocardial infarction, in the adult mammalian heart is unable to compensate its myocardial loss. However, during a transient neonatal period, *i.e.* first week, complete healing of the heart is achieved in mice [114]. Several injury models such as apical ventricular resection, cryoinjury and left coronary artery occlusion have been reported, displaying all of them a characteristic healing pattern [115–117]; an early inflammatory response is firstly activated, followed by a fibrous extracellular matrix deposition phase that allows to maintain the cardiac structural and functional integrity that is finally followed by a resolution phase that promotes myocardial cell division and fibrous scar clearance (see for a recent review; [118]). Thus, multiple cell types are required to heal the damaged heart, including the epicardial and myocardial layers, as well as fibroblasts and macrophages. Understanding of the molecular mechanisms driving cardiac regeneration has greatly advanced over the last decade [119,120], including the functional role of non-coding RNAs such as microRNAs [121–123] and lncRNAs [124–128], particularly with emphasis on cardiomyocyte recovery. In our study we explored the plausible contribution of *Gm14014* during cardiac injury by generating embryonic and postnatal *ex vivo* cryoinjury models. *Gm14014* upregulation is observed in all embryonic stages tested as early as E10.5 when the embryonic heart is formed by epicardial, myocardial and endocardial cells in the absence of a structured fibroskeleton and resident immune cells, supporting the notion that it should be upregulated in one of these three layers. On the other hand, *Gm14014* is down-regulated at P1 stage, when all previously cited cell types are already present. Curiously, activation of distinct signaling pathways including epicardial activation (*Wt1, Tbx18, Tcf21*), and epithelial-to-mesenchymal transition (EMT) (*Snail1, Snail2, Cdh5*) is prominently observed at P1 cryoinjured hearts but not at early embryonic stages (E10.5 and E13.5) supporting a negative correlation between *Gm14014* up-regulation and the onset of these biological processes. Such negative correlation is also observed at P7, since those genes involved in the signaling pathways mentioned above are also down-regulated while *Gm14014* is upregulated, similarly as in the embryonic stages. Therefore, these data support a plausible role of *Gm14014* in cardiac regeneration provided its complementary pattern after cryoinjury in P1 (regenerative) and P7 (non-regenerate) stages [82].

LncRNAs can modulate multiple biological processes, including epigenetic, transcriptional and post-transcriptional processes [48,71,90]. Dissecting their subcellular localization and searching for protein partners can provide further evidence of their functional roles [48,71,90]. We demonstrated herein by RT-qPCR as well as by SCRINSHOT that *Gm14014* is widely expressed in different tissues and cell types. Within the cardiovascular context, its expression is prominently observed in MEC1 epicardial and MEVEC endocardial cells as compared to HL1 myocardial cells and furthermore its subcellular localization in all these cell types is prominently nuclear. Furthermore, functional *in vitro* analyses demonstrated that *Gm14014* is essential for epicardial cell migration, but not for endocardial and myocardial migration, supporting a cell-type specific role. While a large body of evidence is currently reported on the role of lncRNA in oncogenic cell migration and metastasis (see for recent reviews; [129–131]), this is, to the best of our knowledge the first evidence of the functional role of a lncRNA in homeostatic cell migration, with implication for embryonic epicardial development.

Mechanistically, the identification of *Gm14014*-associated proteins by MS revealed a similar number of nuclear, cytoplasmic and nuclear/cytoplasmic proteins. Silencing assays demonstrate that several cytoskeletal proteins such as Myh9 and Myl9 are severely impaired, supporting a plausible molecular link to impaired epicardial cell migration [85,132–134]. However, it remains to be reconciled why *Gm14014* is primarily localized in the nucleus but cytoskeletal reorganization is observed. A plausible explanation is that immature *Gm14014* transcripts are retained into the nucleus

Preprints.org (www.preprints.org) | NOT PEER-REVIEWED | Posted: 2 August 2024 doi:10.20944/preprints202408.0067.v1

and only a subset is selectively translocated towards the cytoplasm exerting its functional role [90], a process that might be developmentally and transcriptionally dynamic. This is indeed in line with the fact that chicken *Gm14014* homologue lncRNA subcellular expression, *i.e. Wt1_76127*, during epicardial and myocardial maturation, progressively becomes more abundantly expressed in the cytoplasm as development proceeds. Similar observation has also been reported for other lncRNAs during development [66,105].

Alternatively, *Gm14014* can interact with nuclearly located proteins that transcriptionally control the expression of key master genes regulating actin cytoskeletal proteins, since also multiple nuclear proteins were detected in our MS analyses. We tested whether Rac1 might be this linking factor, but failed to demonstrate *Gm14014* physical interaction nor immunocytochemical differences. Thus, it might be plausible that *Gm14014* might be interacting with proteins that are both nuclear and cytoplasmic. We provided evidence that *Gm14014* physically interacts with Myl9. Furthermore, we demonstrated that inhibition of *Gm14014* selectively translocates Myl9 to the cytoplasm and additionally diminished *Myh9* expression, a downregulation that is selectively observed only in MEC1 epicardial cells where migration is also halted by *Gm14014* silencing but not in other cell types. Therefore, these observation supports a working model by which Gm14014 physically interacts with Myl9 in the nucleus, facilitating *Myh9* transcription and thus modulating cell migration as previously reported [85] (Figure 6). In absence of *Gm14014*, Myl9 translocates to the cytoplasm and thus does no longer promotes *Myh9* transcription. As a consequence, *Myh9* is downregulated in the cytoplasm and furthermore, leading to cytoskeleton remodeling and thus halting cell migration (Figure 6). Surprisingly, such molecular mechanisms are not observed in the chicken *Gm14014* homologue, *i.e. Wt1_76127*, demonstrating divergent functional roles.

In summary, we provide herein evidence that chicken *Wt1_76127* lncRNA and its murine homologue, *i.e. Gm14014*, display similar tissue distribution profile in embryonic and adult stages. However, transcriptional regulation by key cardiac enriched transcription factors display conserved and divergent profiles. Additionally, we demonstrated that murine *Gm14014*, but not chicken *Wt1_76127* is essential for epicardial, but not myocardial, cell migration, a process that is modulated by *Gm14014*-Myl9 physical interaction and subsequent nuclear-to-cytoplasmic translocation and cytoskeletal re-arrangement. Thus, these data support the notion that homologues lncRNAs can exert distinct and species-specific functional capabilities.

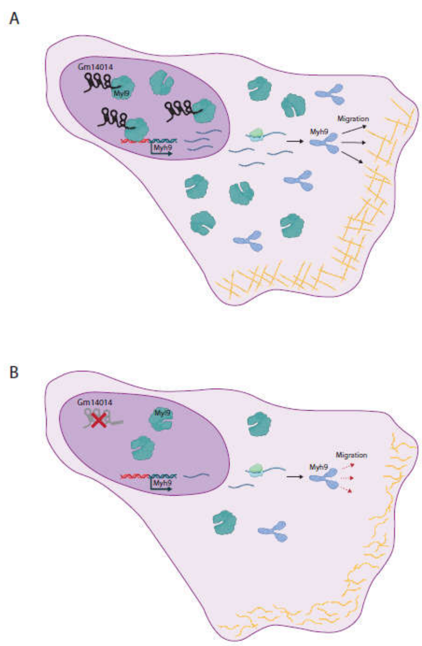

Figure 6. Schematic representation of the working model of *Gm14014* during epicardial cell migration. Panel A illustrate the role of *Gm14014* in homeostasis and Panel B in *Gm14014* silencing assays. Note that *Gm14014* is bound to Myl9 in the nucleus, providing clues to cell migration by interacting with

Preprints.org (www.preprints.org) | NOT PEER-REVIEWED | Posted: 2 August 2024 doi:10.20944/preprints202408.0067.v1

Myh9 in the cytoplasm, while if *Gm14014* is knockdown, no Myl9 nuclear binding occurs and thus is completely translocated to the cytoplasm.

4. Conclusions

We provided herein evidence that chicken *Wt1_76127* and its mouse homologue *Gm14014* are widely distributed in different embryonic and adult tissues, displaying a prominent nuclear localization. Transcriptional regulation of these lncRNAs is exerted by distinct cardiac enriched transcription factors revealing divergent functionalities in chicken and mice. Furthermore, *Gm14014* is distinctly regulated in cryoinjured explants from postnatal mice with (P1) vs without (P7) regenerative capacity, postulating a plausible role for this lncRNA in cardiac regeneration. Mechanistically, *Gm14014* is required for epicardial cell migration, a process mediated by partnering with Myl9, but not *Wt1_76127*, highlighting such evolutionary differences. Thus our data demonstrate a pivotal role for *Gm14014* lncRNA in cell migration, a biological process that is pivotal during cardiac regeneration.

5. Methods

5.1. Chicken Embryonic Tissues and Epicardial Explants

Fertilized eggs from white Leghorn chickens (Granja Santa Isabel, Córdoba, Spain) were incubated at 37.5°C and 50% humidity for 2–7 days. Embryos were harvested at different developmental stages (HH17, HH24 and HH32) and classified according to Hamburger and Hamilton [56]. Embryos were removed from the egg by cutting the blastocyst margin with iridectomy scissors and placed into phosphate-buffered saline (PBS). For RT-qPCR analyses, HH17 PE were dissected out, pooled (n=10), and stored at -80°C until used. Additionally, *in vitro* explants cultures, HH24 and HH32 cardiac explants were cultured for 24 hours and subsequently the ventricular and epicardial outgrowths were separated, isolated, pooled (n=10), and stored at -80°C until used.

5.2. Chicken Primary Cultures

HH36 embryonic hearts were isolated and disintegrated with iridectomy scissors and placed in PBS. The tissues were incubated with trypsin for 30 minutes at 37°C and the supernatant was collected. This trypsinization step was repeated until all the tissue was fully dissociated. The supernatant was centrifugated and the pellet was cultured in plastic Petri dishes with fibroblast culture medium (Dulbecco’s Modified Eagle’s Medium-high glucose) (Sigma) supplemented with fetal bovine serum (FBS) 10%. Two pre-plating steps were made to separate cardiac fibroblasts (CFs) and cardiomyocytes (CMs). Subsequently, CMs from supernatant was cultured in a plastic Petri dish with fresh CMs culture medium supplemented with 0,001M 5-bromo-2-deoxyuridine (Sigma) to inhibit fibroblast proliferation as previously reported [57].

5.3. Mouse Embryonic Tissues

CD1 mice were bred and embryos were collected at different embryonic developmental stages, including embryonic day (E) E10.5, E13.5 and E19.5. Postnatal day (P1, P7 and P21) hearts were also collected. Pregnant females and neonatal mice were euthanized by cervical dislocation and by decapitation, respectively. Subsequently, embryonic and postnatal tissues were dissected, pooled and stored at -80°C until used. Approved consent of the Andalusian Ethic Committee was obtained prior to the initiation of the study.

5.4. Mouse Explants for Cryoinjury

Embryonic hearts for different developmental stages (E10.5, E13.5 and E19.5) and postnatal hearts (P1 and P7) were collected. Apical ventricular sections were isolated and dissected using dissection forceps and micro-scalpel and cultured in multi-wells plates with DMEM/F-12 + GlutaMAX 1 (1X) (Gibco) as culture medium. Apical ventricular explants were cryoinjured using a needle frozen with liquid nitrogen and were cultivated at different times (6, 12, 24 and 48 hours). The explants were collected and stored at -80°C until used.

5.5. Nucleus/Cytoplasm SUBCELLULAR isolation

Cytoplasmic and nuclear RNA fractions from HH17 PE, HH24 and HH32 epicardial/ myocardial outgrowths as well as from primary chicken cardiomyocytes, HL1 cardiomyocytes (SCC065, Sigma-Aldrich), MEVEC endocardial cells [58], MEC1 (SCC187, Sigma-Aldrich) and EPIC epicardial cells [59] were isolated with Cytoplasmic & Nuclear RNA Purification Kit (Norgen, Belmont, CA, USA) following the manufacturer's instructions. After RNA isolation, RT-qPCR analysis for nuclearly enriched *Xist* (isoform 2) mRNA and cytoplasmic *Gapdh* mRNA were performed to validate enrichment on each subcellular fraction. RT-qPCR analysis of distinct lncRNAs was subsequently performed as detailed below.

5.6. siRNA Cell Transfections

Chicken ventricular and epicardial explants, HL1 cardiomyocytes, MEVEC endocardial cells, MEC1 and EPIC epicardial cells (6×10^5 cells per well) were transfected with Pitx2c-siRNA, Srf-siRNA, Nkx2.5-siRNA, Mef2c-siRNA and Myl9-siRNA (Sigma, Aldrich, Munich, Germany), respectively, as previously described [60–62]. siRNA sequences are provided in Supplementary Table S1.

5.7. ASO Design and Transfection

Antisense oligonucleotides (ASOs) were designed as previously reported [63]. The structure of ASOs used in this report consist of a main backbone (10 nucleotides) with phosphorothioate groups, and on both sides 5 nucleotides with different methyl groups**.** ASO transfections were carried out with Lipofectamine 2000 (Invitrogen, Carlsbad, CA, USA) following the manufacturer's guidelines. A concentration of 20nM of *Wt1_76127* and *Gm14014* ASO was applied to the cells at different times, respectively while for *Myl9* ASO the concentration used was 80nM. ASOs sequences are provided in Supplementary Table S1.

5.8. Cell Viability Assays

Cell viability was analyzed with Apoptosis/Necrosis Assay Kit (Abcam), following the manufacturer's instructions. Cell cultures were analyzed using a Leica TCS SP5 II confocal scanning laser microscope. Viable cells were detected with Cytocalcein violet 450 reagent (blue), apoptotic cells with Apopxin Deep Red (red) and apoptotic and necrotic cells were detected with Nuclear Green DCS1 reagent (green).

5.9. Cell Migration Assays

Cell migration was analyzed by scratch assay, as described by Ascione *et al.* [64]. Primary chicken cardiomyocytes, HL1 cardiomyocytes, MEVEC endocardial cells and MEC1 epicardial cells were plated on 24-well culture dishes at a density of 6×10^5 cells per well and incubated until 90-100% confluence. Cell monolayers were manually scratched with a p200 pipette tip. PBS was used to wash the cells and subsequently replaced by the serum-free medium. The experimental group was treated with lipidic vesicles containing ASOs as cargo, while the control group was treated with empty lipidic vesicles, respectively. All plates were photographed after 24 h. In addition, a time lapse analysis was carried out for the two conditions. Cell monolayers were scratched, transfected and cultured for 24h taking pictures every 15 minutes. A Leica TCS SP5 II confocal microscope was used, maintaining optimal temperature and humidity conditions for cell growth.

 doi:10.20944/preprints202408.0067.v1

5.10. Growth Factors and Thymosin β4 Administration

HL1 cardiomyocytes, MEVEC endocardial cells and MEC1 epicardial cells were treated for 24 h with Bmp2, Bmp4, Fgf2, Fgf8 and thymosin β4 (Prospec, East Brunswick, NJ, USA), respectively, as reported by Dueñas *et al.* [55]. Cells were collected and processed according for RT-qPCR. In all cases, 3–5 independent biological replicates were analyzed.

5.11. Immunohistochemical Analyses

Control and experimental treated cells were collected after the corresponding treatment, rinsed in PBS for 10 min and fixed with 4 % PFA for 10 minutes at room temperature. After fixation, the samples were rinsed three times (10 min each) in PBS at room temperature and then permeabilized with 1% Triton X-100 and NH_4Cl 50nM in PBS for 10 min at room temperature. To block nonspecific binding sites, PBS containing gelatin solution 0,2% (Sigma) was applied twice (10 min each). After blocking, the samples were rinsed three times (10 min each) in PBS at room temperature and were immunofluorescently labeled to detect different proteins. Primary antibodies against Actn1 (ab68194, Abcam), Actn4 (ab108198, Abcam), Myh9 (ab75590, Abcam), pHH3 (CA-92590, Milipore), Myl9 (sc-28329, Santa Cruz), Rac1 (sc-514583, Santa Cruz) and MF20 (ATCC) were used, diluted (1:200) in blocking solution, and applied to each culture overnight at 4°C, respectively. Subsequently, the samples were rinsed three times (10 min each) in PBS to remove excess of primary antibody and incubated 30 min at room temperature with Alexa-Fluor 546, 488 and 633 (1:100; Invitrogen) as a secondary antibody, respectively, as corresponding. Finally, the cells were incubated with DAPI (1:2000; Sigma) for 10 min at room temperature and rinsed three times in PBS for 5 min each. Cell cultures were stored in PBS in darkness at 4°C until analyzed using a Leica TCS SP5 II confocal scanning laser microscope.

5.12. SCRINSHOT In Situ Hybridization

SCRINSHOT (*(Single-Cell Resolution IN Situ Hybridization On Tissues)* assay was conducted as described by Sountoulidis *et al*. [65]. Heart tissue from mouse embryos (E14.5) and postnatal 21 days (P21) animals were collected, washed in PBS 1X (pH=7.4), embedded in OCT (FSC22 Clear, Leica), and stored at -80°C until used. 5µm thick cryostat sections were obtained (Leica CM3050S). Padlock probes (40-45 nucleotides) were designed using PrimerQuest online tool (IDT: Integrated DNA Technologies). These DNA oligos were used to design the fluorophore detection oligos, replacing 2-3 "T" nucleotides with "U" to subsequently remove these oligos after the detection cycle using the enzyme Uracil-DNA Glycosylase (Thermo, EN0362). The sequences of the padlock probes and the fluorophore detection oligos are provided in Supplementary Table S1. Images were obtained using a Zeiss Axio Observer Z.2 fluorescent microscope. Image analysis was based on the nuclear segmentation and alignment of the different detection cycles for the genes of interest. Colocalization was obtained as the number of positive cells for the gene of interest relative to the total number of cells in each sample. Further image processing was carried out using FIJI, Cell Profiler, RStudio and TissUUmaps software.

5.13. RNA Isolation and cDNA Synthesis

Total RNA was isolated Direct-Zol RNA Miniprep Kit (Zymo Research), according to the manufacturer's instructions. In all cases, at least three distinct pooled samples were used to perform the corresponding RT-qPCR experiments. For mRNA expression measurements, reverse transcription Maxima First Strand cDNA Synthesis Kit for RT-qPCR (Thermo Scientific) was used, according to the manufacturer's guidelines. Negative controls to assess genomic contamination were performed for each sample, without reverse transcriptase, which resulted in all cases in no detectable amplification product.

 doi:10.20944/preprints202408.0067.v1

5.14. qPCR Analyses (mRNA and lncRNA)

Real-time PCR experiments were performed with 2µL of diluted cDNA, GoTaq® qPCR Master Mix (Promega) and corresponding primer sets described in Supplementary Table S1. All qPCRs were performed using a CFX384TM thermocycler (Bio-Rad) following the manufacturer's recommendations. The relative level of expression of each gene was calculated as described by Livak & Schmittgen [66] using *Gapdh* as an internal control for mRNA expression analyses. All primers were designed to span exon-exon boundaries using the online Primer3 software Primer3Plus (https://www.bioinformatics.nl/cgi-bin/primer3plus/primer3plus.cgi). Each PCR reaction was carried out in triplicate and repeated in at least three distinct biological samples to obtain representative means. No amplifications were observed in PCR control reactions containing only water as template.

5.15. LncRNA Pull Down Assays

Pull down of biotinylated RNA was carried out as described by Panda *et al.* [67]. Biotinylated RNA of exon 1 and exon 2 of *Gm14014* and *Gapdh* were synthesized from PCR fragments using specific forward primers that contained the T7 RNA polymerase promoter sequence [(T7) AGTAATACGACTCACTATAGGG]. Seven fragments were obtained for the sequence of *Gm14014* and one fragment for *Gapdh*. The fragments were biotinylated with Biotin-14-CTP (Thermo Fisher Scientific, Invitrogen) and transcribed with MaxiScript T7 kit (Thermo Fisher Scientific, Invitrogen). Whole-cell lysates (500 µg) from MEC1 cells were incubated with 1 µg of biotinylated RNA (biotinylated *Gm14014* and *Gapdh* samples) for 2h at room temperature. An input sample incubated only with cell lysate was included as a negative control. Complexes were isolated with Streptavidin-coupled Dynabeads (Invitrogen) and analyzed by mass spectrometry (MS). DAVID database and Gene Ontology analyses were subsequently performed on the resulting proteomic data.

5.16. Western Blot

Western blot (WB) was performed with 10% of the pull-down lysate to validate the interaction between *Gm14014*, Myl9 and Rac1. The primary antibodies Myl9 (sc-28329, Santa Cruz) and Rac1 (sc-514583, Santa Cruz) were used at a concentration of 1:100 incubated for 5h at room temperature and the secondary antibody-HRP conjugate (170-6516, Biorad) at 1:5000 for 30 min at room temperature. Blocking was carried out with albumin and washes with PBST, according to the antibody manufacturer's recommendations.

5.17. Statistical Analyses

For statistical analyses of datasets, unpaired Student's t-tests were used. Significance levels or P values are stated in each corresponding figure legend. $P < 0.05$ was considered statistically significant.

Supplementary Materials: The following supporting information can be downloaded at the website of this paper posted on Preprints.org. Figure S1: Panel A. RT-qPCR validation of *Mef2c*, *Nkx2.5*, *Pitx2c* and *Srf* siRNA inhibition in epicardial/ventricular samples, respectively. Panel B. RT-qPCR analyses of *Wt1_76127*, *Bmp4_53170* and *Fgf8_57126* nuclear and cytoplasmic expression in controls and *Mef2c* siRNAs treated of HH24 and HH32 epicardial/ventricular tissues, respectively. Note that inhibition of *Mef2c* selectively modulates nuclear and cytoplasmic expression in different tissues and stages; Figure S2: Panel A. Graphical representation of the secondary structure of *Wt1_76127* lncRNA. Panel B. Graphical representation of the secondary structure of *Gm14014* lncRNA. Red areas in *Gm14014* correspond to the conserved nucleotide sequences in *Wt1_76127*. The colour of nucleotides represents the probability of base pairs; Figure S3: Panel A. RT-qPCR validation of *Xist2* expression as a nuclear marker in nuclear and cytoplasmic extracts of HL1 cardiomyocytes, MEC1 and EPIC epicardial cells and MEVEC endocardial cells, respectively. Panel B. RT-qPCR validation of *Mef2c*, *Nkx2.5*, *Pitx2c* and *Srf* siRNA inhibition and overexpression in HL1 cardiomyocytes, MEC1 and EPIC epicardial cells and MEVEC endocardial cells, respectively. Panel C. Global view of SCRINSHOT in situ

 doi:10.20944/preprints202408.0067.v1

hybridization analyses of *Gm14014* in E14.5 mouse hearts. Global view of SCRINSHOT in situ hybridization analyses of *Gm14014* in P21 ventricular (1) and atrial (2) close-ups. Panel D. Quantitative analysis of SCRINSHOT in situ hybridization for *Gm14014* expression in E14.5 and P21 samples. Note that *Gm14014* expression is higher in embryonic stage than P21; Figure S4: RT-qPCR analyses of *Gm14014, Tnnt2, Wt1, Tbx18, Tcf21, Snail1, Snail2* and *Cdh5* in E10.5, E13.5, E19.5, P1 and P7 cryoinjured hearts as compared to controls. These data represent those plotted in Figure 3 heatmap (panel 3C); Figure S5: Panel A. Schematic representation of the gene ontology analyses corresponding to the biological processes of the *Gm14014* interacting proteins as revealed by RNA pull-down assays and mass spectrometry identification. Panel B. Schematic representation of the gene ontology analyses corresponding to cellular components of the *Gm14014* interacting proteins as revealed by RNA pull-down assays and mass spectrometry identification. Panel C. Schematic representation of the gene ontology analyses corresponding to the molecular functions of the *Gm14014* interacting proteins as revealed by RNA pull-down assays and mass spectrometry identification; Figure S6: Panel A. RT-qPCR validation analyses of *Gm14014* after ASO administration, corresponding to ASO1, ASO2 and ASO1+ASO2 conditions, respectively. Panel B. Schematic representation of the direction of epicardial MEC1 cells in the migration assay between control condition and *Gm14014* ASO treatment. These data represent the graph in Figure 4 (panel 4D). Panel C. RT-qPCR validation analysis of *Myl9* after siRNA and ASO of *Myl9* administration. Panel D and E. Representative immunocytochemical images of Myh9 and Myl9 expression corresponding to HL1 cardiomyocytes after 6h (panel D) and 24h (panel E) ASO1 administration, respectively and their corresponding quantitative analyses graphs. Observe that no significant differences are observed at any of the two distinct timepoints analyzed; Figure S7: Panel A. Schematic representation *in ovo* of *Wt1_76127* ASO pericardial administration in HH17 chicken embryos. Panel B. Graphical representation of the survival rate in controls and HH17 *Wt1_76127* ASO treated embryos. Panel C. Graphical representation of the beats per minute frequency in controls and HH17 *Wt1_76127* ASO treated embryos. Panel D. Graphical representation of cardiac rhythm rhythmicity in controls and HH17 *Wt1_76127* ASO treated embryos. Panel E. Graphical representation of heart surface in controls and HH17 *Wt1_76127* ASO treated embryos. Observe that none of the parameters analyzed is significantly different between controls and HH17 *Wt1_76127* ASO treated embryos; Table S1: List of the nucleotide sequences corresponding to RT-qPCR primers, biotinylated RNAS primers for RNA pulldown assays, siRNAs, antisense oligonucleotides (ASOs), SCRINSHOT padlock probes and SCRINSHOT detection oligonucleotides; Table S2: Comparative analyses of nucleotide conservation between the chicken *Wt1_76127* lncRNA and the mouse *Gm14014* lncRNA; Table S3: List of *Gm14014* associated proteins as revealed by RNA pulldown assays and mass spectrometry identification.

Author Contributions: All authors contributed to the study conception and design. Material preparation, data collection and analysis were performed by S.C-C, C.G-P and E. L-V. The first draft of the manuscript was written by DF and all authors commented on previous versions of the manuscript. All authors have read and approved the final manuscript.

Funding: This work was supported by grants of the Ministerio de Innovación y Ciencia of the Spanish Government to DF (PID2022-138163OB-C32) and of the Consejería de Universidad, Investigación e Innovación of the Junta de Andalucia Regional Council to DF (ProyExcel_00409).

Institutional Review Board Statement: This study was performed in line with the principles of the Declaration of Helsinki. Approval was granted by the Ethics Committee of the University of Jaén (code 14/03/2022/038).

Data Availability: The datasets generated during and/or analysed during the current study are available from the corresponding author on reasonable request.

Acknowledgments: We would like to thank the excellent technical support of the CICT-Universidad de Jaén. We would like to thank Jose Luis de la Pompa (CNIC, Madrid) for sharing MEVEC cells. We would like to thank Oscar Ocaña for critical reading of the manuscript.

Competing interests: The authors declare that they have no competing interest.

Preprints.org (www.preprints.org) | NOT PEER-REVIEWED | Posted: 2 August 2024 doi:10.20944/preprints202408.0067.v1

Abbreviations

ASO	antisense oligonucleotides
Bmp	Bone morphogenetic protein
cDNA	complementary DNA
CFs	cardiac fibroblasts
CMs	cardiomyocytes
EE	embryonic epicardium
EMT	epithelial to mesenchymal transition
EPDCs	epicardial derived cells
FBS	Fetal bovine serum
Fgf	Fibroblast growth factor
GO	gene ontology
HH	Hamburger & Hamilton
HRP	horseradish peroxidase
lncRNA	long non coding RNA
PBS	phosphate buffer saline
PBST	phosphate buffer saline with Tris
PE	proepicardium
RT-qPCR	reverse transcriptase-quantitative polymerase chain reaction
SCRINSHOT	Single Cell resolution in situ hybridization on tissues

References

1. Moorman AF, Christoffels VM. Cardiac chamber formation: development, genes, and evolution. Physiol Rev. 2003 Oct;83(4):1223-67. doi: 10.1152/physrev.00006.2003. PMID: 14506305.
2. Campione M, Franco D. Current Perspectives in Cardiac Laterality. J Cardiovasc Dev Dis. 2016 Dec 9;3(4):34. doi: 10.3390/jcdd3040034. PMID: 29367577; PMCID: PMC5715725.
3. Dueñas A, Aranega AE, Franco D. More than Just a Simple Cardiac Envelope; Cellular Contributions of the Epicardium. Front Cell Dev Biol. 2017 May 1;5:44. doi: 10.3389/fcell.2017.00044. PMID: 28507986; PMCID: PMC5410615.
4. Männer J, Schlueter J, Brand T. Experimental analyses of the function of the proepicardium using a new microsurgical procedure to induce loss-of-proepicardial-function in chick embryos. Dev Dyn. 2005 Aug;233(4):1454-63. doi: 10.1002/dvdy.20487. PMID: 15977171.
5. Pérez-Pomares JM, Macías D, García-Garrido L, Muñoz-Chápuli R. The origin of the subepicardial mesenchyme in the avian embryo: an immunohistochemical and quail-chick chimera study. Dev Biol. 1998 Aug 1;200(1):57-68. doi: 10.1006/dbio.1998.8949. PMID: 9698456.
6. Pérez-Pomares JM, Phelps A, Sedmerova M, Carmona R, González-Iriarte M, Muñoz-Chápuli R, Wessels A. Experimental studies on the spatiotemporal expression of WT1 and RALDH2 in the embryonic avian heart: a model for the regulation of myocardial and valvuloseptal development by epicardially derived cells (EPDCs). Dev Biol. 2002 Jul 15;247(2):307-26. doi: 10.1006/dbio.2002.0706. PMID: 12086469.
7. Lie-Venema H, van den Akker NM, Bax NA, Winter EM, Maas S, Kekarainen T, Hoeben RC, deRuiter MC, Poelmann RE, Gittenberger-de Groot AC. Origin, fate, and function of epicardium-derived cells (EPDCs) in normal and abnormal cardiac development. ScientificWorldJournal. 2007 Nov 12;7:1777-98. doi: 10.1100/tsw.2007.294. PMID: 18040540; PMCID: PMC5901302.
8. Gittenberger-de Groot AC, Winter EM, Poelmann RE. Epicardium-derived cells (EPDCs) in development, cardiac disease and repair of ischemia. J Cell Mol Med. 2010 May;14(5):1056-60. doi: 10.1111/j.1582-4934.2010.01077.x. PMID: 20646126; PMCID: PMC3822740.
9. Cano E, Carmona R, Ruiz-Villalba A, Rojas A, Chau YY, Wagner KD, Wagner N, Hastie ND, Muñoz-Chápuli R, Pérez-Pomares JM. Extracardiac septum transversum/proepicardial endothelial cells pattern

 doi:10.20944/preprints202408.0067.v1

embryonic coronary arterio-venous connections. Proc Natl Acad Sci U S A. 2016 Jan 19;113(3):656-61. doi: 10.1073/pnas.1509834113. Epub 2016 Jan 6. PMID: 26739565; PMCID: PMC4725486.

10. Kruithof BP, van Wijk B, Somi S, Kruithof-de Julio M, Pérez Pomares JM, Weesie F, Wessels A, Moorman AF, van den Hoff MJ. BMP and FGF regulate the differentiation of multipotential pericardial mesoderm into the myocardial or epicardial lineage. Dev Biol. 2006 Jul 15;295(2):507-22. doi: 10.1016/j.ydbio.2006.03.033. Epub 2006 Apr 3. PMID: 16753139.
11. Martínez-Estrada OM, Lettice LA, Essafi A, Guadix JA, Slight J, Velecela V, Hall E, Reichmann J, Devenney PS, Hohenstein P, Hosen N, Hill RE, Muñoz-Chapuli R, Hastie ND. Wt1 is required for cardiovascular progenitor cell formation through transcriptional control of Snail and E-cadherin. Nat Genet. 2010 Jan;42(1):89-93. doi: 10.1038/ng.494. Epub 2009 Dec 20. PMID: 20023660; PMCID: PMC2799392.
12. Velecela V, Torres-Cano A, García-Melero A, Ramiro-Pareta M, Müller-Sánchez C, Segarra-Mondejar M, Chau YY, Campos-Bonilla B, Reina M, Soriano FX, Hastie ND, Martínez FO, Martínez-Estrada OM. Epicardial cell shape and maturation are regulated by Wt1 via transcriptional control of <i>Bmp4</i>. Development. 2019 Oct 17;146(20):dev178723. doi: 10.1242/dev.178723. PMID: 31624071.
13. Wagner N, Wagner KD. Every Beat You Take-The Wilms' Tumor Suppressor WT1 and the Heart. Int J Mol Sci. 2021 Jul 18;22(14):7675. doi: 10.3390/ijms22147675. PMID: 34299295; PMCID: PMC8306835.
14. von Gise A, Zhou B, Honor LB, Ma Q, Petryk A, Pu WT. WT1 regulates epicardial epithelial to mesenchymal transition through β-catenin and retinoic acid signaling pathways. Dev Biol. 2011 Aug 15;356(2):421-31. doi: 10.1016/j.ydbio.2011.05.668. Epub 2011 May 30. PMID: 21663736; PMCID: PMC3147112.
15. Bax NA, van Oorschot AA, Maas S, Braun J, van Tuyn J, de Vries AA, Groot AC, Goumans MJ. In vitro epithelial-to-mesenchymal transformation in human adult epicardial cells is regulated by TGFβ-signaling and WT1. Basic Res Cardiol. 2011 Sep;106(5):829-47. doi: 10.1007/s00395-011-0181-0. Epub 2011 Apr 24. PMID: 21516490; PMCID: PMC3149675.
16. Guadix JA, Ruiz-Villalba A, Lettice L, Velecela V, Muñoz-Chápuli R, Hastie ND, Pérez-Pomares JM, Martínez-Estrada OM. Wt1 controls retinoic acid signalling in embryonic epicardium through transcriptional activation of Raldh2. Development. 2011 Mar;138(6):1093-7. doi: 10.1242/dev.044594. PMID: 21343363; PMCID: PMC3042868.
17. Greulich F, Farin HF, Schuster-Gossler K, Kispert A. Tbx18 function in epicardial development. Cardiovasc Res. 2012 Dec 1;96(3):476-83. doi: 10.1093/cvr/cvs277. Epub 2012 Aug 27. PMID: 22926762.
18. Wu SP, Dong XR, Regan JN, Su C, Majesky MW. Tbx18 regulates development of the epicardium and coronary vessels. Dev Biol. 2013 Nov 15;383(2):307-20. doi: 10.1016/j.ydbio.2013.08.019. Epub 2013 Sep 7. PMID: 24016759; PMCID: PMC4172450.
19. Takeichi M, Nimura K, Mori M, Nakagami H, Kaneda Y. The transcription factors Tbx18 and Wt1 control the epicardial epithelial-mesenchymal transition through bi-directional regulation of Slug in murine primary epicardial cells. PLoS One. 2013;8(2):e57829. doi: 10.1371/journal.pone.0057829. Epub 2013 Feb 28. PMID: 23469079; PMCID: PMC3585213.
20. Lu J, Richardson JA, Olson EN. Capsulin: a novel bHLH transcription factor expressed in epicardial progenitors and mesenchyme of visceral organs. Mech Dev. 1998 Apr;73(1):23-32. doi: 10.1016/s0925-4773(98)00030-6. PMID: 9545521.
21. Robb L, Mifsud L, Hartley L, Biben C, Copeland NG, Gilbert DJ, Jenkins NA, Harvey RP. epicardin: A novel basic helix-loop-helix transcription factor gene expressed in epicardium, branchial arch myoblasts, and mesenchyme of developing lung, gut, kidney, and gonads. Dev Dyn. 1998 Sep;213(1):105-13. doi: 10.1002/(SICI)1097-0177(199809)213:1<105::AID-AJA10>3.0.CO;2-1. PMID: 9733105.
22. Tandon P, Miteva YV, Kuchenbrod LM, Cristea IM, Conlon FL. Tcf21 regulates the specification and maturation of proepicardial cells. Development. 2013 Jun;140(11):2409-21. doi: 10.1242/dev.093385. Epub 2013 May 1. PMID: 23637334; PMCID: PMC3653561.
23. Acharya A, Baek ST, Huang G, Eskiocak B, Goetsch S, Sung CY, Banfi S, Sauer MF, Olsen GS, Duffield JS, Olson EN, Tallquist MD. The bHLH transcription factor Tcf21 is required for lineage-specific EMT of cardiac fibroblast progenitors. Development. 2012 Jun;139(12):2139-49. doi: 10.1242/dev.079970. Epub 2012 May 9. PMID: 22573622; PMCID: PMC3357908.
24. Braitsch CM, Combs MD, Quaggin SE, Yutzey KE. Pod1/Tcf21 is regulated by retinoic acid signaling and inhibits differentiation of epicardium-derived cells into smooth muscle in the developing heart. Dev Biol.

2012 Aug 15;368(2):345-57. doi: 10.1016/j.ydbio.2012.06.002. Epub 2012 Jun 9. PMID: 22687751; PMCID: PMC3414197.
25. Zhou B, von Gise A, Ma Q, Rivera-Feliciano J, Pu WT. Nkx2-5- and Isl1-expressing cardiac progenitors contribute to proepicardium. Biochem Biophys Res Commun. 2008 Oct 24;375(3):450-3. doi: 10.1016/j.bbrc.2008.08.044. Epub 2008 Aug 21. PMID: 18722343; PMCID: PMC2610421.
26. Schlueter J, Brand T. A right-sided pathway involving FGF8/Snai1 controls asymmetric development of the proepicardium in the chick embryo. Proc Natl Acad Sci U S A. 2009 May 5;106(18):7485-90. doi: 10.1073/pnas.0811944106. Epub 2009 Apr 13. PMID: 19365073; PMCID: PMC2678653.
27. Watt AJ, Battle MA, Li J, Duncan SA. GATA4 is essential for formation of the proepicardium and regulates cardiogenesis. Proc Natl Acad Sci U S A. 2004 Aug 24;101(34):12573-8. doi: 10.1073/pnas.0400752101. Epub 2004 Aug 13. PMID: 15310850; PMCID: PMC515098.
28. González-Rosa JM, Peralta M, Mercader N. Pan-epicardial lineage tracing reveals that epicardium derived cells give rise to myofibroblasts and perivascular cells during zebrafish heart regeneration. Dev Biol. 2012 Oct 15;370(2):173-86. doi: 10.1016/j.ydbio.2012.07.007. Epub 2012 Aug 1. PMID: 22877945.
29. Schnabel K, Wu CC, Kurth T, Weidinger G. Regeneration of cryoinjury induced necrotic heart lesions in zebrafish is associated with epicardial activation and cardiomyocyte proliferation. PLoS One. 2011 Apr 12;6(4):e18503. doi: 10.1371/journal.pone.0018503. PMID: 21533269; PMCID: PMC3075262.
30. Lepilina A, Coon AN, Kikuchi K, Holdway JE, Roberts RW, Burns CG, Poss KD. A dynamic epicardial injury response supports progenitor cell activity during zebrafish heart regeneration. Cell. 2006 Nov 3;127(3):607-19. doi: 10.1016/j.cell.2006.08.052. PMID: 17081981.
31. Ito K, Morioka M, Kimura S, Tasaki M, Inohaya K, Kudo A. Differential reparative phenotypes between zebrafish and medaka after cardiac injury. Dev Dyn. 2014 Sep;243(9):1106-15. doi: 10.1002/dvdy.24154. Epub 2014 Jun 25. PMID: 24947076.
32. Wei K, Serpooshan V, Hurtado C, Diez-Cuñado M, Zhao M, Maruyama S, Zhu W, Fajardo G, Noseda M, Nakamura K, Tian X, Liu Q, Wang A, Matsuura Y, Bushway P, Cai W, Savchenko A, Mahmoudi M, Schneider MD, van den Hoff MJ, Butte MJ, Yang PC, Walsh K, Zhou B, Bernstein D, Mercola M, Ruiz-Lozano P. Epicardial FSTL1 reconstitution regenerates the adult mammalian heart. Nature. 2015 Sep 24;525(7570):479-85. doi: 10.1038/nature15372. Epub 2015 Sep 16. PMID: 26375005; PMCID: PMC4762253.
33. Darehzereshki A, Rubin N, Gamba L, Kim J, Fraser J, Huang Y, Billings J, Mohammadzadeh R, Wood J, Warburton D, Kaartinen V, Lien CL. Differential regenerative capacity of neonatal mouse hearts after cryoinjury. Dev Biol. 2015 Mar 1;399(1):91-99. doi: 10.1016/j.ydbio.2014.12.018. Epub 2014 Dec 31. PMID: 25555840; PMCID: PMC4339535.
34. Cai W, Tan J, Yan J, Zhang L, Cai X, Wang H, Liu F, Ye M, Cai CL. Limited Regeneration Potential with Minimal Epicardial Progenitor Conversions in the Neonatal Mouse Heart after Injury. Cell Rep. 2019 Jul 2;28(1):190-201.e3. doi: 10.1016/j.celrep.2019.06.003. PMID: 31269439; PMCID: PMC6837841.
35. Bock-Marquette I, Shrivastava S, Pipes GC, Thatcher JE, Blystone A, Shelton JM, Galindo CL, Melegh B, Srivastava D, Olson EN, DiMaio JM. Thymosin beta4 mediated PKC activation is essential to initiate the embryonic coronary developmental program and epicardial progenitor cell activation in adult mice in vivo. J Mol Cell Cardiol. 2009 May;46(5):728-38. doi: 10.1016/j.yjmcc.2009.01.017. PMID: 19358334; PMCID: PMC2768533.
36. Smart N, Risebro CA, Melville AA, Moses K, Schwartz RJ, Chien KR, Riley PR. Thymosin beta4 induces adult epicardial progenitor mobilization and neovascularization. Nature. 2007 Jan 11;445(7124):177-82. doi: 10.1038/nature05383. Epub 2006 Nov 15. PMID: 17108969.
37. Smart N, Bollini S, Dubé KN, Vieira JM, Zhou B, Davidson S, Yellon D, Riegler J, Price AN, Lythgoe MF, Pu WT, Riley PR. De novo cardiomyocytes from within the activated adult heart after injury. Nature. 2011 Jun 8;474(7353):640-4. doi: 10.1038/nature10188. PMID: 21654746; PMCID: PMC3696525.
38. Smart N, Dubé KN, Riley PR. Epicardial progenitor cells in cardiac regeneration and neovascularisation. Vascul Pharmacol. 2013 Mar;58(3):164-73. doi: 10.1016/j.vph.2012.08.001. Epub 2012 Aug 11. PMID: 22902355.
39. Smart N, Riley PR. The epicardium as a candidate for heart regeneration. Future Cardiol. 2012 Jan;8(1):53-69. doi: 10.2217/fca.11.87. PMID: 22185446; PMCID: PMC3977139.
40. Cao J, Poss KD. The epicardium as a hub for heart regeneration. Nat Rev Cardiol. 2018 Oct;15(10):631-647. doi: 10.1038/s41569-018-0046-4. PMID: 29950578; PMCID: PMC6143401.

 doi:10.20944/preprints202408.0067.v1

41. Saifi O, Ghandour B, Jaalouk D, Refaat M, Mahfouz R. Myocardial regeneration: role of epicardium and implicated genes. Mol Biol Rep. 2019 Dec;46(6):6661-6674. doi: 10.1007/s11033-019-05075-0. Epub 2019 Sep 23. PMID: 31549371.
42. Ruiz-Villalba A, Simón AM, Pogontke C, Castillo MI, Abizanda G, Pelacho B, Sánchez-Domínguez R, Segovia JC, Prósper F, Pérez-Pomares JM. Interacting resident epicardium-derived fibroblasts and recruited bone marrow cells form myocardial infarction scar. J Am Coll Cardiol. 2015 May 19;65(19):2057-66. doi: 10.1016/j.jacc.2015.03.520. PMID: 25975467.
43. Suffee N, Moore-Morris T, Farahmand P, Rücker-Martin C, Dilanian G, Fradet M, Sawaki D, Derumeaux G, LePrince P, Clément K, Dugail I, Puceat M, Hatem SN. Atrial natriuretic peptide regulates adipose tissue accumulation in adult atria. Proc Natl Acad Sci U S A. 2017 Jan 31;114(5):E771-E780. doi: 10.1073/pnas.1610968114. Epub 2017 Jan 17. PMID: 28096344; PMCID: PMC5293064.
44. Shaihov-Teper O, Ram E, Ballan N, Brzezinski RY, Naftali-Shani N, Masoud R, Ziv T, Lewis N, Schary Y, Levin-Kotler LP, Volvovitch D, Zuroff EM, Amunts S, Regev-Rudzki N, Sternik L, Raanani E, Gepstein L, Leor J. Extracellular Vesicles From Epicardial Fat Facilitate Atrial Fibrillation. Circulation. 2021 Jun 22;143(25):2475-2493. doi: 10.1161/CIRCULATIONAHA.120.052009. Epub 2021 Apr 1. PMID: 33793321.
45. Al-Rawahi M, Proietti R, Thanassoulis G. Pericardial fat and atrial fibrillation: Epidemiology, mechanisms and interventions. Int J Cardiol. 2015 Sep 15;195:98-103. doi: 10.1016/j.ijcard.2015.05.129. Epub 2015 May 21. PMID: 26025867.
46. Gaeta M, Bandera F, Tassinari F, Capasso L, Cargnelutti M, Pelissero G, Malavazos AE, Ricci C. Is epicardial fat depot associated with atrial fibrillation? A systematic review and meta-analysis. Europace. 2017 May 1;19(5):747-752. doi: 10.1093/europace/euw398. PMID: 28087595.
47. Bartel DP. Metazoan MicroRNAs. Cell. 2018 Mar 22;173(1):20-51. doi: 10.1016/j.cell.2018.03.006. PMID: 29570994; PMCID: PMC6091663.
48. Mercer TR, Dinger ME, Mattick JS. Long non-coding RNAs: insights into functions. Nat Rev Genet. 2009 Mar;10(3):155-9. doi: 10.1038/nrg2521. PMID: 19188922.
49. Klattenhoff CA, Scheuermann JC, Surface LE, Bradley RK, Fields PA, Steinhauser ML, Ding H, Butty VL, Torrey L, Haas S, Abo R, Tabebordbar M, Lee RT, Burge CB, Boyer LA. Braveheart, a long noncoding RNA required for cardiovascular lineage commitment. Cell. 2013 Jan 31;152(3):570-83. doi: 10.1016/j.cell.2013.01.003. Epub 2013 Jan 24. PMID: 23352431; PMCID: PMC3563769.
50. Grote P, Wittler L, Hendrix D, Koch F, Währisch S, Beisaw A, Macura K, Bläss G, Kellis M, Werber M, Herrmann BG. The tissue-specific lncRNA Fendrr is an essential regulator of heart and body wall development in the mouse. Dev Cell. 2013 Jan 28;24(2):206-14. doi: 10.1016/j.devcel.2012.12.012. PMID: 23369715; PMCID: PMC4149175.
51. Yang L, Deng J, Ma W, Qiao A, Xu S, Yu Y, Boriboun C, Kang X, Han D, Ernst P, Zhou L, Shi J, Zhang E, Li TS, Qiu H, Nakagawa S, Blackshaw S, Zhang J, Qin G. Ablation of lncRNA <i>Miat</i> attenuates pathological hypertrophy and heart failure. Theranostics. 2021 Jul 6;11(16):7995-8007. doi: 10.7150/thno.50990. PMID: 34335976; PMCID: PMC8315059.
52. Di Salvo TG, Guo Y, Su YR, Clark T, Brittain E, Absi T, Maltais S, Hemnes A. Right ventricular long noncoding RNA expression in human heart failure. Pulm Circ. 2015 Mar;5(1):135-61. doi: 10.1086/679721. PMID: 25992278; PMCID: PMC4405709.
53. Wu DM, Zhou ZK, Fan SH, Zheng ZH, Wen X, Han XR, Wang S, Wang YJ, Zhang ZF, Shan Q, Li MQ, Hu B, Lu J, Chen GQ, Hong XW, Zheng YL. Comprehensive RNA-Seq Data Analysis Identifies Key mRNAs and lncRNAs in Atrial Fibrillation. Front Genet. 2019 Oct 2;10:908. doi: 10.3389/fgene.2019.00908. PMID: 31632440; PMCID: PMC6783610.
54. Ke ZP, Xu YJ, Wang ZS, Sun J. RNA sequencing profiling reveals key mRNAs and long noncoding RNAs in atrial fibrillation. J Cell Biochem. 2020 Aug;121(8-9):3752-3763. doi: 10.1002/jcb.29504. Epub 2019 Nov 3. PMID: 31680326.
55. Dueñas A, Expósito A, Muñoz MDM, de Manuel MJ, Cámara-Morales A, Serrano- Osorio F, García-Padilla C, Hernández-Torres F, Domínguez JN, Aránega A, Franco D. MiR-195 enhances cardiomyogenic differentiation of the proepicardium/septum transversum by Smurf1 and Foxp1 modulation. Sci Rep. 2020 Jun 9;10(1):9334. doi: 10.1038/s41598-020-66325-x. PMID: 32518241; PMCID: PMC7283354.
56. Hamburger V, Hamilton HL. A series of normal stages in the development of the chick embryo. 1951. Dev Dyn. 1992 Dec;195(4):231-72. doi: 10.1002/aja.1001950404. PMID: 1304821.

57. Jones SP, Kennedy SW. Chicken embryo cardiomyocyte cultures--a new approach for studying effects of halogenated aromatic hydrocarbons in the avian heart. Toxicol Sci. 2009 May;109(1):66-74. doi: 10.1093/toxsci/kfp039. Epub 2009 Feb 17. PMID: 19223662.
58. D'Amato G, Luxán G, del Monte-Nieto G, Martínez-Poveda B, Torroja C, Walter W, Bochter MS, Benedito R, Cole S, Martinez F, Hadjantonakis AK, Uemura A, Jiménez-Borreguero LJ, de la Pompa JL. Sequential Notch activation regulates ventricular chamber development. Nat Cell Biol. 2016 Jan;18(1):7-20. doi: 10.1038/ncb3280. Epub 2015 Dec 7. PMID: 26641715; PMCID: PMC4816493.
59. Ruiz-Villalba A, Ziogas A, Ehrbar M, Pérez-Pomares JM. Characterization of epicardial-derived cardiac interstitial cells: differentiation and mobilization of heart fibroblast progenitors. PLoS One. 2013;8(1):e53694. doi: 10.1371/journal.pone.0053694. Epub 2013 Jan 18. PMID: 23349729; PMCID: PMC3548895.
60. Lozano-Velasco E, Wangensteen R, Quesada A, Garcia-Padilla C, Osorio JA, Ruiz-Torres MD, Aranega A, Franco D. Hyperthyroidism, but not hypertension, impairs PITX2 expression leading to Wnt-microRNA-ion channel remodeling. PLoS One. 2017 Dec 1;12(12):e0188473. doi: 10.1371/journal.pone.0188473. PMID: 29194452; PMCID: PMC5711019.
61. Lozano-Velasco E, Hernández-Torres F, Daimi H, Serra SA, Herraiz A, Hove-Madsen L, Aránega A, Franco D. Pitx2 impairs calcium handling in a dose-dependent manner by modulating Wnt signalling. Cardiovasc Res. 2016 Jan 1;109(1):55-66. doi: 10.1093/cvr/cvv207. Epub 2015 Aug 4. PMID: 26243430
62. García-Padilla C, Domínguez JN, Lodde V, Munk R, Abdelmohsen K, Gorospe M, Jiménez-Sábado V, Ginel A, Hove-Madsen L, Aránega AE, Franco D. Identification of atrial-enriched lncRNA Walras linked to cardiomyocyte cytoarchitecture and atrial fibrillation. FASEB J. 2022 Jan;36(1):e22051. doi: 10.1096/fj.202100844RR. PMID: 34861058; PMCID: PMC8684585.
63. Le BT, Agarwal S, Veedu RN. Evaluation of DNA segments in 2'-modified RNA sequences in designing efficient splice switching antisense oligonucleotides. RSC Adv. 2021 Apr 13;11(23):14029-14035. doi: 10.1039/d1ra00878a. PMID: 35423918; PMCID: PMC8697723.
64. Ascione F, Vasaturo A, Caserta S, D'Esposito V, Formisano P, Guido S. Comparison between fibroblast wound healing and cell random migration assays in vitro. Exp Cell Res. 2016 Sep 10;347(1):123-132. doi: 10.1016/j.yexcr.2016.07.015. Epub 2016 Jul 27. PMID: 27475838.
65. Sountoulidis A, Liontos A, Nguyen HP, Firsova AB, Fysikopoulos A, Qian X, Seeger W, Sundström E, Nilsson M, Samakovlis C. SCRINSHOT enables spatial mapping of cell states in tissue sections with single-cell resolution. PLoS Biol. 2020 Nov 20;18(11):e3000675. doi: 10.1371/journal.pbio.3000675. PMID: 33216742; PMCID: PMC7717588.
66. Livak KJ, Schmittgen TD. Analysis of relative gene expression data using real-time quantitative PCR and the 2(-Delta Delta C(T)) Method. Methods. 2001 Dec;25(4):402-8. doi: 10.1006/meth.2001.1262. PMID: 11846609.
67. Panda AC, Martindale JL, Gorospe M. Affinity Pulldown of Biotinylated RNA for Detection of Protein-RNA Complexes. Bio Protoc. 2016 Dec 20;6(24):e2062. doi: 10.21769/BioProtoc.2062. PMID: 28516119; PMCID: PMC5431594.
68. Jiang C, Li Y, Zhao Z, Lu J, Chen H, Ding N, Wang G, Xu J, Li X. Identifying and functionally characterizing tissue-specific and ubiquitously expressed human lncRNAs. Oncotarget. 2016 Feb 9;7(6):7120-33. doi: 10.18632/oncotarget.6859. PMID: 26760768; PMCID: PMC4872773.
69. Long Y, Wang X, Youmans DT, Cech TR. How do lncRNAs regulate transcription? Sci Adv. 2017 Sep 27;3(9):eaao2110. doi: 10.1126/sciadv.aao2110. PMID: 28959731; PMCID: PMC5617379.
70. Wang J, Gu J, You A, Li J, Zhang Y, Rao G, Ge X, Zhang K, Li J, Liu X, Wang Q, Lin T, Cheng L, Zhu M, Wu X, Wang D. The transcription factor USF1 promotes glioma cell invasion and migration by activating lncRNA HAS2-AS1. Biosci Rep. 2020 Aug 28;40(8):BSR20200487. doi: 10.1042/BSR20200487. PMID: 32776110; PMCID: PMC7442972.
71. Mattick JS, Amaral PP, Carninci P, Carpenter S, Chang HY, Chen LL, Chen R, Dean C, Dinger ME, Fitzgerald KA, Gingeras TR, Guttman M, Hirose T, Huarte M, Johnson R, Kanduri C, Kapranov P, Lawrence JB, Lee JT, Mendell JT, Mercer TR, Moore KJ, Nakagawa S, Rinn JL, Spector DL, Ulitsky I, Wan Y, Wilusz JE, Wu M. Long non-coding RNAs: definitions, functions, challenges and recommendations. Nat Rev Mol Cell Biol. 2023 Jan 3. doi: 10.1038/s41580-022-00566-8. Epub ahead of print. PMID: 36596869.
72. Wang J, Zohar R, McCulloch CA. Multiple roles of alpha-smooth muscle actin in mechanotransduction. Exp Cell Res. 2006 Feb 1;312(3):205-14. doi: 10.1016/j.yexcr.2005.11.004. Epub 2005 Dec 2. PMID: 16325810.

73. Xia Y, Duca S, Perder B, Dündar F, Zumbo P, Qiu M, Yao J, Cao Y, Harrison MRM, Zangi L, Betel D, Cao J. Activation of a transient progenitor state in the epicardium is required for zebrafish heart regeneration. Nat Commun. 2022 Dec 13;13(1):7704. doi: 10.1038/s41467-022-35433-9. PMID: 36513650; PMCID: PMC9747719.
74. Lacraz GPA, Junker JP, Gladka MM, Molenaar B, Scholman KT, Vigil-Garcia M, Versteeg D, de Ruiter H, Vermunt MW, Creyghton MP, Huibers MMH, de Jonge N, van Oudenaarden A, van Rooij E. Tomo-Seq Identifies SOX9 as a Key Regulator of Cardiac Fibrosis During Ischemic Injury. Circulation. 2017 Oct 10;136(15):1396-1409. doi: 10.1161/CIRCULATIONAHA.117.027832. Epub 2017 Jul 19. PMID: 28724751.
75. Garcia-Padilla C, Hernandez-Torres F, Lozano-Velasco E, Dueñas A, Muñoz-Gallardo MDM, Garcia-Valencia IS, Palencia-Vincent L, Aranega A, Franco D. The Role of Bmp- and Fgf Signaling Modulating Mouse Proepicardium Cell Fate. Front Cell Dev Biol. 2022 Jan 4;9:757781. doi: 10.3389/fcell.2021.757781. PMID: 35059396; PMCID: PMC8763981.
76. Dergilev KV, Shevchenko EK, Tsokolaeva ZI, Beloglazova IB, Zubkova ES, Boldyreva MA, Menshikov MY, Ratner EI, Penkov D, Parfyonova YV. Cell Sheet Comprised of Mesenchymal Stromal Cells Overexpressing Stem Cell Factor Promotes Epicardium Activation and Heart Function Improvement in a Rat Model of Myocardium Infarction. Int J Mol Sci. 2020 Dec 16;21(24):9603. doi: 10.3390/ijms21249603. PMID: 33339427; PMCID: PMC7766731.
77. Dergilev KV, Tsokolaeva ZI, Beloglazova IB, Ratner EI, Parfenova EV. Transforming Growth Factor Beta (TGF-β1) Induces Pro-Reparative Phenotypic Changes in Epicardial Cells in Mice. Bull Exp Biol Med. 2021 Feb;170(4):565-570. doi: 10.1007/s10517-021-05107-5. Epub 2021 Mar 17. PMID: 33730328.
78. van Wijk B, Gunst QD, Moorman AF, van den Hoff MJ. Cardiac regeneration from activated epicardium. PLoS One. 2012;7(9):e44692. doi: 10.1371/journal.pone.0044692. Epub 2012 Sep 20. PMID: 23028582; PMCID: PMC3447884.
79. Lepilina A, Coon AN, Kikuchi K, Holdway JE, Roberts RW, Burns CG, Poss KD. A dynamic epicardial injury response supports progenitor cell activity during zebrafish heart regeneration. Cell. 2006 Nov 3;127(3):607-19. doi: 10.1016/j.cell.2006.08.052. PMID: 17081981.
80. Mercer SE, Odelberg SJ, Simon HG. A dynamic spatiotemporal extracellular matrix facilitates epicardial-mediated vertebrate heart regeneration. Dev Biol. 2013 Oct 15;382(2):457-69. doi: 10.1016/j.ydbio.2013.08.002. Epub 2013 Aug 11. PMID: 23939298; PMCID: PMC3957425.
81. Schnabel K, Wu CC, Kurth T, Weidinger G. Regeneration of cryoinjury induced necrotic heart lesions in zebrafish is associated with epicardial activation and cardiomyocyte proliferation. PLoS One. 2011 Apr 12;6(4):e18503. doi: 10.1371/journal.pone.0018503. PMID: 21533269; PMCID: PMC3075262.
82. Liu C, Wang L, Wang X, Hou X. A complete heart regeneration model with inflammation as a key component. Exp Anim. 2021 Nov 10;70(4):479-487. doi: 10.1538/expanim.20-0191. Epub 2021 Jun 15. PMID: 34135270; PMCID: PMC8614014.
83. Ribeiro DM, Zanzoni A, Cipriano A, Delli Ponti R, Spinelli L, Ballarino M, Bozzoni I, Tartaglia GG, Brun C. Protein complex scaffolding predicted as a prevalent function of long non-coding RNAs. Nucleic Acids Res. 2018 Jan 25;46(2):917-928. doi: 10.1093/nar/gkx1169. PMID: 29165713; PMCID: PMC5778612.
84. Luo J, Qu L, Gao F, Lin J, Liu J, Lin A. LncRNAs: Architectural Scaffolds or More Potential Roles in Phase Separation. Front Genet. 2021 Mar 31;12:626234. doi: 10.3389/fgene.2021.626234. PMID: 33868368; PMCID: PMC8044363.
85. Luo XG, Zhang CL, Zhao WW, Liu ZP, Liu L, Mu A, Guo S, Wang N, Zhou H, Zhang TC. Histone methyltransferase SMYD3 promotes MRTF-A-mediated transactivation of MYL9 and migration of MCF-7 breast cancer cells. Cancer Lett. 2014 Mar 1;344(1):129-137. doi: 10.1016/j.canlet.2013.10.026. Epub 2013 Nov 1. PMID: 24189459.
86. Chan TC, Pan CT, Hsieh HY, Vejvisithsakul PP, Wei RJ, Yeh BW, Wu WJ, Chen LR, Shiao MS, Li CF, Shiue YL. The autocrine glycosylated-GREM1 interacts with TGFB1 to suppress TGFβ/BMP/SMAD-mediated EMT partially by inhibiting MYL9 transactivation in urinary carcinoma. Cell Oncol (Dordr). 2023 Aug;46(4):933-951. doi: 10.1007/s13402-023-00788-8. Epub 2023 Mar 15. PMID: 36920729.
87. Jiang C, Li Y, Zhao Z, Lu J, Chen H, Ding N, Wang G, Xu J, Li X. Identifying and functionally characterizing tissue-specific and ubiquitously expressed human lncRNAs. Oncotarget. 2016 Feb 9;7(6):7120-33. doi: 10.18632/oncotarget.6859. PMID: 26760768; PMCID: PMC4872773.
88. Gomes AQ, Nolasco S, Soares H. Non-coding RNAs: multi-tasking molecules in the cell. Int J Mol Sci. 2013 Jul 31;14(8):16010-39. doi: 10.3390/ijms140816010. PMID: 23912238; PMCID: PMC3759897.

89. Kaushik K, Leonard VE, Kv S, Lalwani MK, Jalali S, Patowary A, Joshi A, Scaria V, Sivasubbu S. Dynamic expression of long non-coding RNAs (lncRNAs) in adult zebrafish. PLoS One. 2013 Dec 31;8(12):e83616. doi: 10.1371/journal.pone.0083616. PMID: 24391796; PMCID: PMC3877055.
90. Statello L, Guo CJ, Chen LL, Huarte M. Gene regulation by long non-coding RNAs and its biological functions. Nat Rev Mol Cell Biol. 2021 Feb;22(2):96-118. doi: 10.1038/s41580-020-00315-9. Epub 2020 Dec 22. Erratum in: Nat Rev Mol Cell Biol. 2021 Jan 8;: PMID: 33353982; PMCID: PMC7754182.
91. Martin JF, Schwarz JJ, Olson EN. Myocyte enhancer factor (MEF) 2C: a tissue- restricted member of the MEF-2 family of transcription factors. Proc Natl Acad Sci U S A. 1993 Jun 1;90(11):5282-6. doi: 10.1073/pnas.90.11.5282. PMID: 8506376; PMCID: PMC46700.
92. Edmondson DG, Lyons GE, Martin JF, Olson EN. Mef2 gene expression marks the cardiac and skeletal muscle lineages during mouse embryogenesis. Development. 1994 May;120(5):1251-63. doi: 10.1242/dev.120.5.1251. PMID: 8026334.
93. Lin Q, Schwarz J, Bucana C, Olson EN. Control of mouse cardiac morphogenesis and myogenesis by transcription factor MEF2C. Science. 1997 May 30;276(5317):1404-7. doi: 10.1126/science.276.5317.1404. PMID: 9162005; PMCID: PMC4437729.
94. Yamagishi H, Yamagishi C, Nakagawa O, Harvey RP, Olson EN, Srivastava D. The combinatorial activities of Nkx2.5 and dHAND are essential for cardiac ventricle formation. Dev Biol. 2001 Nov 15;239(2):190-203. doi: 10.1006/dbio.2001.0417. PMID: 11784028.
95. Lyons I, Parsons LM, Hartley L, Li R, Andrews JE, Robb L, Harvey RP. Myogenic and morphogenetic defects in the heart tubes of murine embryos lacking the homeo box gene Nkx2-5. Genes Dev. 1995 Jul 1;9(13):1654-66. doi: 10.1101/gad.9.13.1654. PMID: 7628699.
96. Biben C, Weber R, Kesteven S, Stanley E, McDonald L, Elliott DA, Barnett L, Köentgen F, Robb L, Feneley M, Harvey RP. Cardiac septal and valvular dysmorphogenesis in mice heterozygous for mutations in the homeobox gene Nkx2-5. Circ Res. 2000 Nov 10;87(10):888-95. doi: 10.1161/01.res.87.10.888. PMID: 11073884.
97. Wang D, Chang PS, Wang Z, Sutherland L, Richardson JA, Small E, Krieg PA, Olson EN. Activation of cardiac gene expression by myocardin, a transcriptional cofactor for serum response factor. Cell. 2001 Jun 29;105(7):851-62. doi: 10.1016/s0092-8674(01)00404-4. PMID: 11439182.
98. Li L, Liu Z, Mercer B, Overbeek P, Olson EN. Evidence for serum response factor-mediated regulatory networks governing SM22alpha transcription in smooth, skeletal, and cardiac muscle cells. Dev Biol. 1997 Jul 15;187(2):311-21. doi: 10.1006/dbio.1997.8621. PMID: 9242426.
99. Kitamura K, Miura H, Miyagawa-Tomita S, Yanazawa M, Katoh-Fukui Y, Suzuki R, Ohuchi H, Suehiro A, Motegi Y, Nakahara Y, Kondo S, Yokoyama M. Mouse Pitx2 deficiency leads to anomalies of the ventral body wall, heart, extra- and periocular mesoderm and right pulmonary isomerism. Development. 1999 Dec;126(24):5749-58. doi: 10.1242/dev.126.24.5749. PMID: 10572050.
100. Campione M, Steinbeisser H, Schweickert A, Deissler K, van Bebber F, Lowe LA, Nowotschin S, Viebahn C, Haffter P, Kuehn MR, Blum M. The homeobox gene Pitx2: mediator of asymmetric left-right signaling in vertebrate heart and gut looping. Development. 1999 Mar;126(6):1225-34. doi: 10.1242/dev.126.6.1225. PMID: 10021341.
101. Campione M, Ros MA, Icardo JM, Piedra E, Christoffels VM, Schweickert A, Blum M, Franco D, Moorman AF. Pitx2 expression defines a left cardiac lineage of cells: evidence for atrial and ventricular molecular isomerism in the iv/iv mice. Dev Biol. 2001 Mar 1;231(1):252-64. doi: 10.1006/dbio.2000.0133. PMID: 11180966.
102. Franco D, Campione M. The role of Pitx2 during cardiac development. Linking left-right signaling and congenital heart diseases. Trends Cardiovasc Med. 2003 May;13(4):157-63. doi: 10.1016/s1050-1738(03)00039-2. PMID: 12732450.
103. Zhou B, von Gise A, Ma Q, Rivera-Feliciano J, Pu WT. Nkx2-5- and Isl1-expressing cardiac progenitors contribute to proepicardium. Biochem Biophys Res Commun. 2008 Oct 24;375(3):450-3. doi: 10.1016/j.bbrc.2008.08.044. Epub 2008 Aug 21. PMID: 18722343; PMCID: PMC2610421.
104. van Wijk B, van den Berg G, Abu-Issa R, Barnett P, van der Velden S, Schmidt M, Ruijter JM, Kirby ML, Moorman AF, van den Hoff MJ. Epicardium and myocardium separate from a common precursor pool by crosstalk between bone morphogenetic protein- and fibroblast growth factor-signaling pathways. Circ Res. 2009 Aug 28;105(5):431-41. doi: 10.1161/CIRCRESAHA.109.203083. Epub 2009 Jul 23. PMID: 19628790; PMCID: PMC2861358.

105. Schlueter J, Brand T. A right-sided pathway involving FGF8/Snai1 controls asymmetric development of the proepicardium in the chick embryo. Proc Natl Acad Sci U S A. 2009 May 5;106(18):7485-90. doi: 10.1073/pnas.0811944106. Epub 2009 Apr 13. PMID: 19365073; PMCID: PMC2678653.
106. Männer J. Spontaneous Left Cardiac Isomerism in Chick Embryos: Case Report, Review of the Literature, and Possible Significance for the Understanding of Ventricular Non-Compaction Cardiomyopathy in the Setting of Human Heterotaxy Syndromes. J Cardiovasc Dev Dis. 2019 Nov 8;6(4):40. doi: 10.3390/jcdd6040040. PMID: 31717331; PMCID: PMC6955803.
107. Phan D, Rasmussen TL, Nakagawa O, McAnally J, Gottlieb PD, Tucker PW, Richardson JA, Bassel-Duby R, Olson EN. BOP, a regulator of right ventricular heart development, is a direct transcriptional target of MEF2C in the developing heart. Development. 2005 Jun;132(11):2669-78. doi: 10.1242/dev.01849. PMID: 15890826.
108. Liu ZP, Nakagawa O, Nakagawa M, Yanagisawa H, Passier R, Richardson JA, Srivastava D, Olson EN. CHAMP, a novel cardiac-specific helicase regulated by MEF2C. Dev Biol. 2001 Jun 15;234(2):497-509. doi: 10.1006/dbio.2001.0277. PMID: 11397016.
109. Zou Y, Evans S, Chen J, Kuo HC, Harvey RP, Chien KR. CARP, a cardiac ankyrin repeat protein, is downstream in the Nkx2-5 homeobox gene pathway. Development. 1997 Feb;124(4):793-804. doi: 10.1242/dev.124.4.793. PMID: 9043061.
110. Nakashima Y, Ono K, Yoshida Y, Kojima Y, Kita T, Tanaka M, Kimura T. The search for Nkx2-5-regulated genes using purified embryonic stem cell-derived cardiomyocytes with Nkx2-5 gene targeting. Biochem Biophys Res Commun. 2009 Dec 18;390(3):821-6. doi: 10.1016/j.bbrc.2009.10.056. Epub 2009 Oct 15. PMID: 19836354.
111. García-Padilla C, Domínguez JN, Aránega AE, Franco D. Differential chamber-specific expression and regulation of long non-coding RNAs during cardiac development. Biochim Biophys Acta Gene Regul Mech. 2019 Oct;1862(10):194435. doi: 10.1016/j.bbagrm.2019.194435. Epub 2019 Nov 1. PMID: 31678627.
112. Choi M, Lu YW, Zhao J, Wu M, Zhang W, Long X. Transcriptional control of a novel long noncoding RNA Mymsl in smooth muscle cells by a single Cis-element and its initial functional characterization in vessels. J Mol Cell Cardiol. 2020 Jan;138:147-157. doi: 10.1016/j.yjmcc.2019.11.148. Epub 2019 Nov 18. PMID: 31751568; PMCID: PMC7036038.
113. Zhang Q, Song C, Zhang M, Liu Y, Wang L, Xie Y, Qi H, Ba L, Shi P, Cao Y, Sun H. Super-enhancer-driven lncRNA Snhg7 aggravates cardiac hypertrophy via Tbx5/GLS2/ferroptosis axis. Eur J Pharmacol. 2023 Aug 15;953:175822. doi: 10.1016/j.ejphar.2023.175822. Epub 2023 Jun 3. PMID: 37277029.
114. Porrello ER, Mahmoud AI, Simpson E, Hill JA, Richardson JA, Olson EN, Sadek HA. Transient regenerative potential of the neonatal mouse heart. Science. 2011 Feb 25;331(6020):1078-80. doi: 10.1126/science.1200708. PMID: 21350179; PMCID: PMC3099478.
115. González-Rosa JM, Mercader N. Cryoinjury as a myocardial infarction model for the study of cardiac regeneration in the zebrafish. Nat Protoc. 2012 Mar 29;7(4):782-8. doi: 10.1038/nprot.2012.025. PMID: 22461067.
116. IJ, Sanz-Morejón A, Mercader N. Ventricular Cryoinjury as a Model to Study Heart Regeneration in Zebrafish. Methods Mol Biol. 2021;2158:51-62. doi: 10.1007/978-1-0716-0668-1_5. Erratum in: Methods Mol Biol. 2021;2158:C1. PMID: 32857365.
117. Mahmoud AI, Porrello ER, Kimura W, Olson EN, Sadek HA. Surgical models for cardiac regeneration in neonatal mice. Nat Protoc. 2014 Feb;9(2):305-11. doi: 10.1038/nprot.2014.021. Epub 2014 Jan 16. PMID: 24434799; PMCID: PMC3977725.
118. Caño-Carrillo S, Lozano-Velasco E, Castillo-Casas JM, Sánchez-Fernández C, Franco D. The Role of ncRNAs in Cardiac Infarction and Regeneration. J Cardiovasc Dev Dis. 2023 Mar 15;10(3):123. doi: 10.3390/jcdd10030123. PMID: 36975887; PMCID: PMC10052289.
119. Uygur A, Lee RT. Mechanisms of Cardiac Regeneration. Dev Cell. 2016 Feb 22;36(4):362-74. doi: 10.1016/j.devcel.2016.01.018. PMID: 26906733; PMCID: PMC4768311.
120. Costa A, Cushman S, Haubner BJ, Derda AA, Thum T, Bär C. Neonatal injury models: integral tools to decipher the molecular basis of cardiac regeneration. Basic Res Cardiol. 2022 May 3;117(1):26. doi: 10.1007/s00395-022-00931-w. PMID: 35503383; PMCID: PMC9064850.
121. Raso A, Dirkx E, Sampaio-Pinto V, El Azzouzi H, Cubero RJ, Sorensen DW, Ottaviani L, Olieslagers S, Huibers MM, de Weger R, Siddiqi S, Moimas S, Torrini C, Zentillin L, Braga L, Nascimento DS, da Costa Martins PA, van Berlo JH, Zacchigna S, Giacca M, De Windt LJ. A microRNA program regulates the balance

between cardiomyocyte hyperplasia and hypertrophy and stimulates cardiac regeneration. Nat Commun. 2021 Aug 10;12(1):4808. doi: 10.1038/s41467-021-25211-4. Erratum in: Nat Commun. 2022 Aug 25;13(1):4977. PMID: 34376683; PMCID: PMC8355162.

122. Eulalio A, Mano M, Dal Ferro M, Zentilin L, Sinagra G, Zacchigna S, Giacca M. Functional screening identifies miRNAs inducing cardiac regeneration. Nature. 2012 Dec 20;492(7429):376-81. doi: 10.1038/nature11739. Epub 2012 Dec 5. PMID: 23222520.
123. Del Campo CV, Liaw NY, Gunadasa-Rohling M, Matthaei M, Braga L, Kennedy T, Salinas G, Voigt N, Giacca M, Zimmermann WH, Riley PR. Regenerative potential of epicardium-derived extracellular vesicles mediated by conserved miRNA transfer. Cardiovasc Res. 2022 Jan 29;118(2):597-611. doi: 10.1093/cvr/cvab054. PMID: 33599250; PMCID: PMC8803084.
124. Li M, Zheng H, Han Y, Chen Y, Li B, Chen G, Chen X, Huang S, He X, Wei G, Xu T, Feng X, Liao W, Liao Y, Chen Y, Bin J. LncRNA Snhg1-driven self-reinforcing regulatory network promoted cardiac regeneration and repair after myocardial infarction. Theranostics. 2021 Sep 13;11(19):9397-9414. doi: 10.7150/thno.57037. PMID: 34646377; PMCID: PMC8490501.
125. Fu W, Ren H, Shou J, Liao Q, Li L, Shi Y, Jose PA, Zeng C, Wang WE. Loss of NPPA-AS1 promotes heart regeneration by stabilizing SFPQ-NONO heteromer-induced DNA repair. Basic Res Cardiol. 2022 Mar 5;117(1):10. doi: 10.1007/s00395-022-00921-y. PMID: 35247074.
126. Ponnusamy M, Liu F, Zhang YH, Li RB, Zhai M, Liu F, Zhou LY, Liu CY, Yan KW, Dong YH, Wang M, Qian LL, Shan C, Xu S, Wang Q, Zhang YH, Li PF, Zhang J, Wang K. Long Noncoding RNA CPR (Cardiomyocyte Proliferation Regulator) Regulates Cardiomyocyte Proliferation and Cardiac Repair. Circulation. 2019 Jun 4;139(23):2668-2684. doi: 10.1161/CIRCULATIONAHA.118.035832. Epub 2019 Mar 5. PMID: 30832495.
127. Cai B, Ma W, Ding F, Zhang L, Huang Q, Wang X, Hua B, Xu J, Li J, Bi C, Guo S, Yang F, Han Z, Li Y, Yan G, Yu Y, Bao Z, Yu M, Li F, Tian Y, Pan Z, Yang B. The Long Noncoding RNA CAREL Controls Cardiac Regeneration. J Am Coll Cardiol. 2018 Jul 31;72(5):534-550. doi: 10.1016/j.jacc.2018.04.085. Epub 2018 Jul 2. PMID: 30056829.
128. Chen YM, Li H, Fan Y, Zhang QJ, Li X, Wu LJ, Chen ZJ, Zhu C, Qian LM. Identification of differentially expressed lncRNAs involved in transient regeneration of the neonatal C57BL/6J mouse heart by next-generation high-throughput RNA sequencing. Oncotarget. 2017 Apr 25;8(17):28052-28062. doi:10.18632/oncotarget.15887. PMID: 28427208; PMCID: PMC5438630
129. Liu SJ, Dang HX, Lim DA, Feng FY, Maher CA. Long noncoding RNAs in cancer metastasis. Nat Rev Cancer. 2021 Jul;21(7):446-460. doi: 10.1038/s41568-021-00353-1. Epub 2021 May 5. PMID: 33953369; PMCID: PMC8288800.
130. Schmitt AM, Chang HY. Long Noncoding RNAs in Cancer Pathways. Cancer Cell. 2016 Apr 11;29(4):452-463. doi: 10.1016/j.ccell.2016.03.010. PMID: 27070700; PMCID: PMC4831138.
131. Ahmad M, Weiswald LB, Poulain L, Denoyelle C, Meryet-Figuiere M. Involvement of lncRNAs in cancer cells migration, invasion and metastasis: cytoskeleton and ECM crosstalk. J Exp Clin Cancer Res. 2023 Jul 18;42(1):173. doi: 10.1186/s13046-023-02741-x. PMID: 37464436; PMCID: PMC10353155.
132. Yang B, Liu H, Bi Y, Cheng C, Li G, Kong P, Zhang L, Shi R, Zhang Y, Zhang R, Cheng X. MYH9 promotes cell metastasis <i>via</i> inducing Angiogenesis and Epithelial Mesenchymal Transition in Esophageal Squamous Cell Carcinoma. Int J Med Sci. 2020 Jul 25;17(13):2013-2023. doi: 10.7150/ijms.46234. PMID: 32788880; PMCID: PMC7415390.
133. Wen B, Luo L, Zeng Z, Luo X. <i>MYL9</i> promotes squamous cervical cancer migration and invasion by enhancing aerobic glycolysis. J Int Med Res. 2023 Nov;51(11):3000605231208582. doi: 10.1177/03000605231208582. PMID: 37950670; PMCID: PMC10640809.
134. Feng M, Dong N, Zhou X, Ma L, Xiang R. Myosin light chain 9 promotes the proliferation, invasion, migration and angiogenesis of colorectal cancer cells by binding to Yes-associated protein 1 and regulating Hippo signaling. Bioengineered. 2022 Jan;13(1):96-106. doi: 10.1080/21655979.2021.2008641. PMID: 34974798; PMCID: PMC8805887.